The Geometry of a Gabbro Unit Intruded in a Granitic Body, Billdal, Sweden

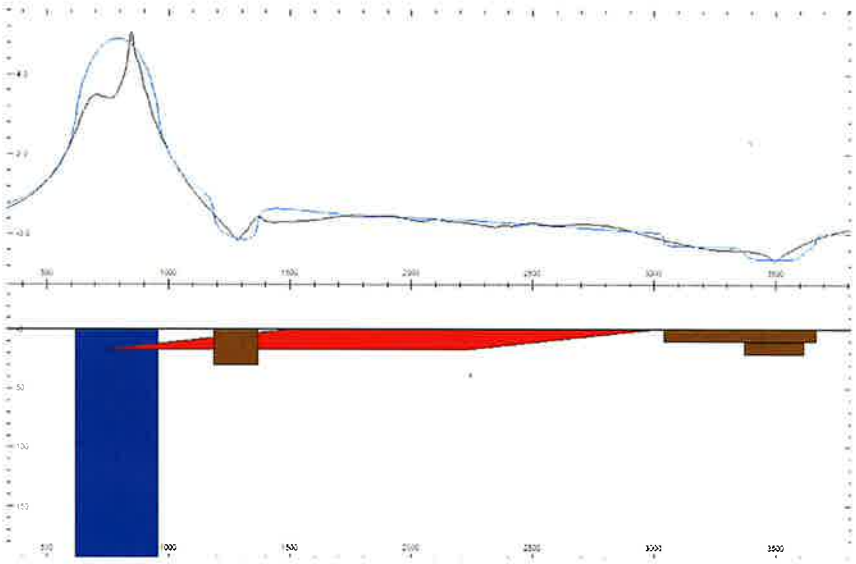

Helge V. Birgerheim

Degree of Bachelor of Science
with a major in Earth Sciences
15 hec

Department of Earth Sciences
University of Gothenburg
2023 B-1243

Faculty of Science

UNIVERSITY OF GOTHENBURG

UNIVERSITY OF GOTHENBURG
Department of Earth Sciences
Geovetarcentrum/Earth Science Centre

The Geometry of a Gabbro Unit Intruded in a Granitic Body, Billdal, Sweden

Helge V. Birgerheim

ISSN 1400-3821

B1243
Bachelor of Science thesis
Göteborg 2023

Mailing address
Geovetarcentrum
S 405 30 Göteborg

Address
Geovetarcentrum
Guldhedsgatan 5A

Telephone
031-786 19 56

Geovetarcentrum
Göteborg University
S-405 30 Göteborg
SWEDEN

Table of Content

Abstract

The Billdal area is a part of the Kungsbacka bimodal suite characterized by alternating felsic and mafic intrusions in a N-S trending band stretching from Kungsbacka in the south to Trollhättan in the north. The aim of this study is to better understand the large-scale geometries of one of these gabbro intrusions in a 25 km^2 area around Billdal and Hällesås, south-western Sweden. To do this, a gravimetric survey is conducted in order to interpolate the gravity anomalies over a wider area. A profile of this interpolation is compared with a simulated gravity profile in ModelVision. A bedrock profile based on mapped outcrops is also created to verify the result and to attempt to calculate the shape of the intrusion. The gravity simulation shows all the signs of being a deep magma conduit and an almost horizontal sill, but the density of the theorized magma conduit needs to be higher than previously assumed. No gravitational signs of a massive gabbro structure can be found over the area presumed to house the sill, and no other magma conduits have been identified in the study area. The bedrock profile indicates the same structure as the simulated gravity profile.

Introduction

The survey area lies in the southern part of the Idefjorden terrane (Fig. 1), which forms part of the Sweconorwegian belt. The target is a granitic and a gabbroitic rock unit belonging to the Kungsbacka bimodal suite. As it contains dense gabbro and light granite but no intermediate rock units with densities in between the two, it is suitable for gravity surveying.

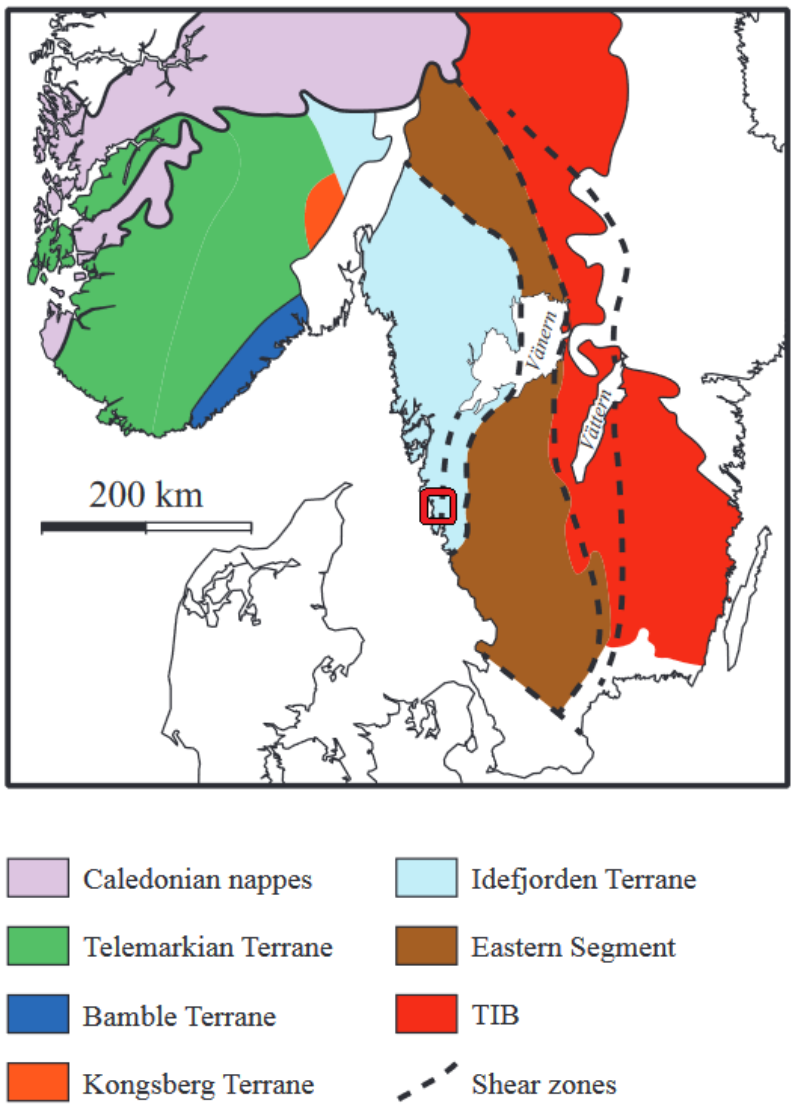

Figure 1: Geological map showing the different tectonic units in the Sweconorwegian belt (Berthelsen 1980; Bingen et al., 2008). From Sturkell & Hegardt, 2020.

The bimodal Billdal–Hällesås intrusion is located 1-3 km east of Billdal, 20 km south of Gothenburg (Fig. 2).
The rock units here are separated by a significant density contrast, and they barely have any magnetic properties. As the magnetic susceptibility is low for both units a magnetic survey will not give any useful results. Additionally, several large power lines cross the study area both over and under the ground. This leaves gravimetry as the only geophysical method to help explore the extent of the gabbro beneath the surface. Furthermore, the Swedish geodetic survey (SGU) hosts maps over the local geology and gravity anomalies over the area (SGU, 2023). The SGU gravity anomaly map indicates a positive anomaly on the western side of road 158 (Fig. 3). The location of this gravity anomaly was confirmed by Tormos (2021) (Fig. 4). Unfortunately, neither the SGU gravity anomaly map nor their bedrock map contains any information of observation points. However, the gravity map shows a positive anomaly in an area where the SGU geological map does not indicate any major gabbro body. The prominent surface gabbro body is instead located to the east of road 158 (Fig. 2).

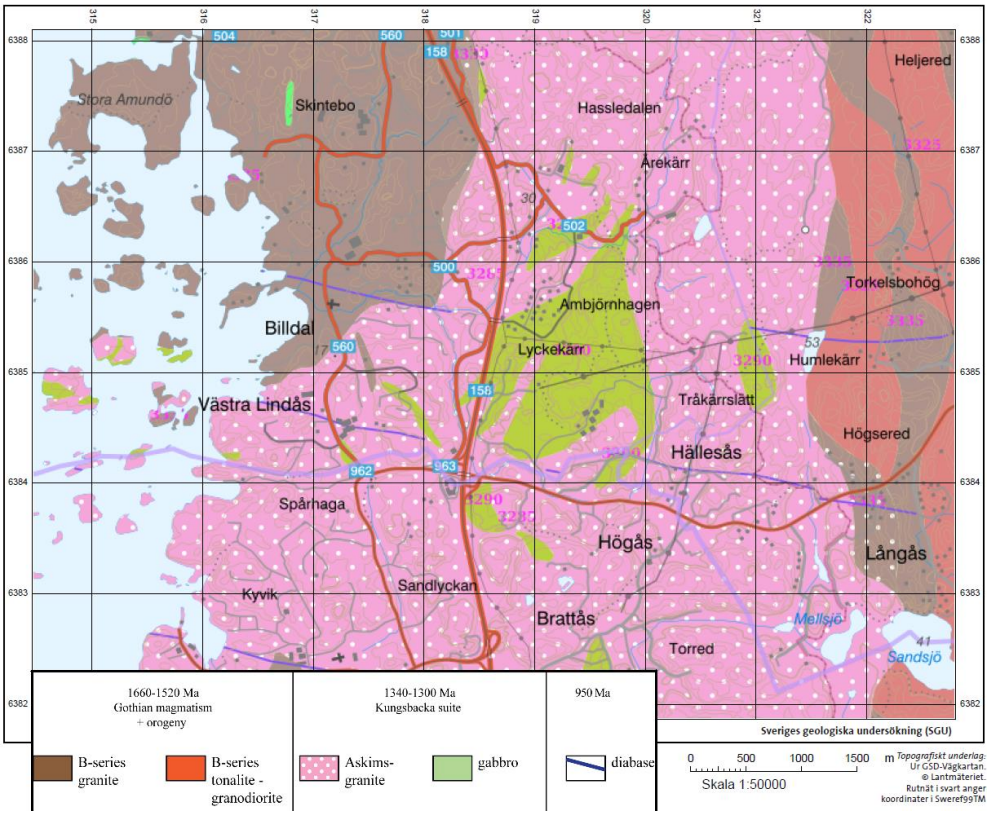

Figure 2: Bedrock map showing the bimodal intrusion in the Billdal – Hällesås area. From SGU.

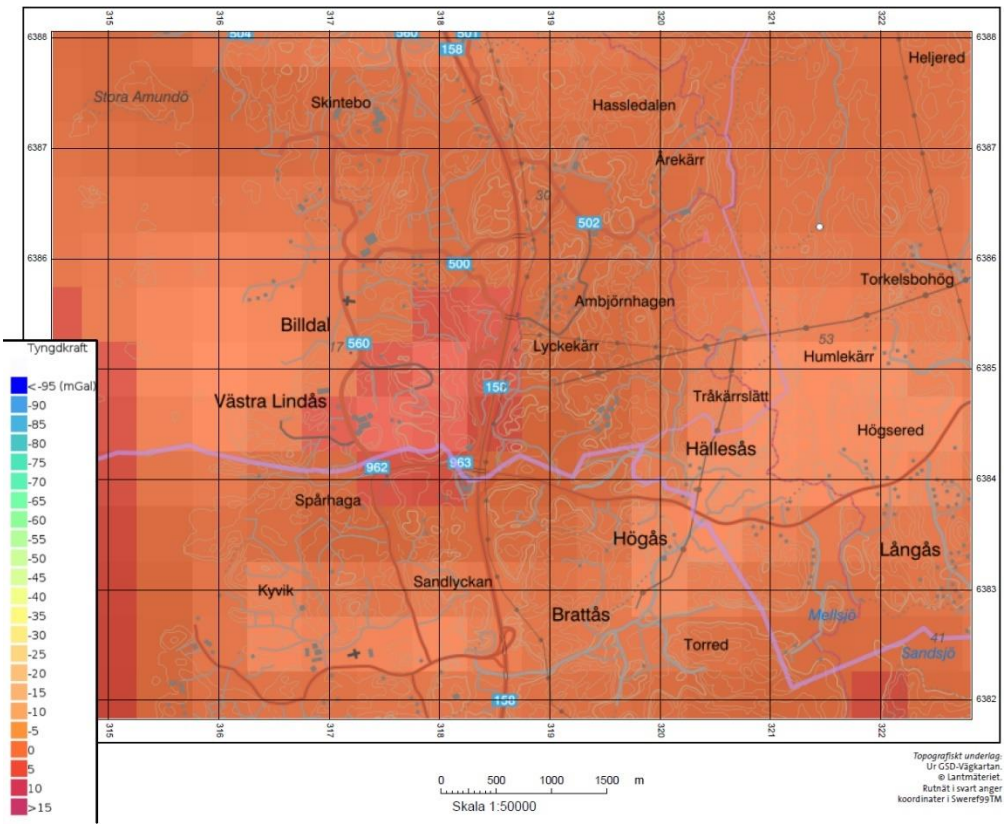

Figure 3: 500x500 m gravitational anomaly map over the bimodal intrusion in the Billdal–Hällesås area. The red-pink spot west of road 158 signifies a positive gravity anomaly. Note that the scale shows the high values at the bottom and the low values at the top. From SGU.

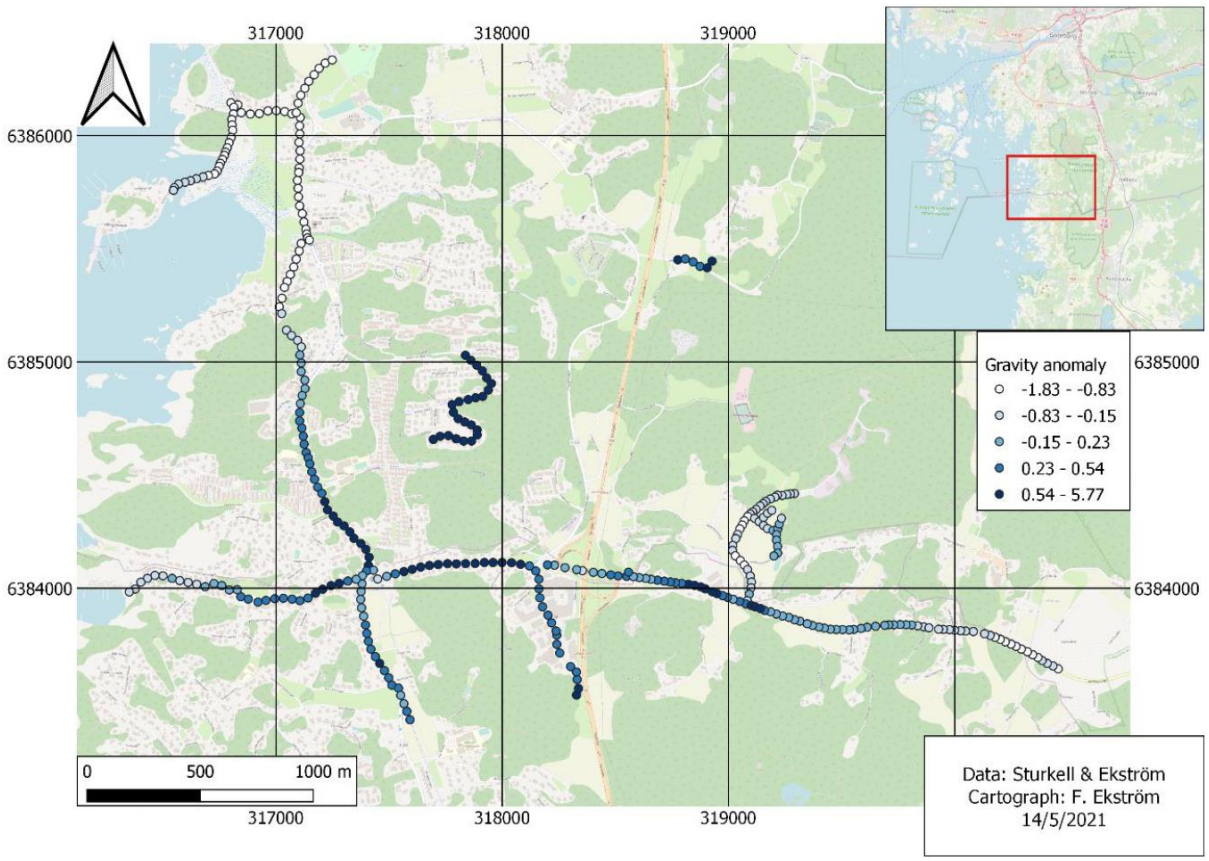

Figure 4: Map of the gravity anomaly measurements used by Tormos (2021). The raw data can be found in appendix II. Figure from Tormos, 2021

Geological history

The geology of southwestern Sweden is generally dominated by gneisses and granites (Fig. 5). Billdal is located in the Kungsbacka bimodal suite, which lies in the granitic and granodioritic part of the Idefjorden terrane which formed 1.5-1,6 Ga ago during the Gothian orogeny. The Kungsbacka bimodal suite consists of multiple intrusions of alternating granites and gabbro stretching north to south in a band from Trollhättan to Kungsbacka. Based on U-Pb dating on these granites by Hegardt et al (2006), the granites of the Kungsbacka bimodal suite intruded ~200 Ma after the median and western segments of the Idefjord terrain cooled. The Kungsbacka bimodal suite runs along the Göta älv shear zone, which also form the boundary between the median and western segment. Bands of bimodal intrusions are one of very few signs left of extensive volcanism in deeply eroded bedrock (Vladimirov et al., 2013). Bimodal volcanism is generally associated with rift settings. Signs of widespread north-south trending rifting in the young Idefjorden terrane post 1,5 Ga is supported by Åhäll & Connelly (2007), although the cause of rifting is not entirely known.

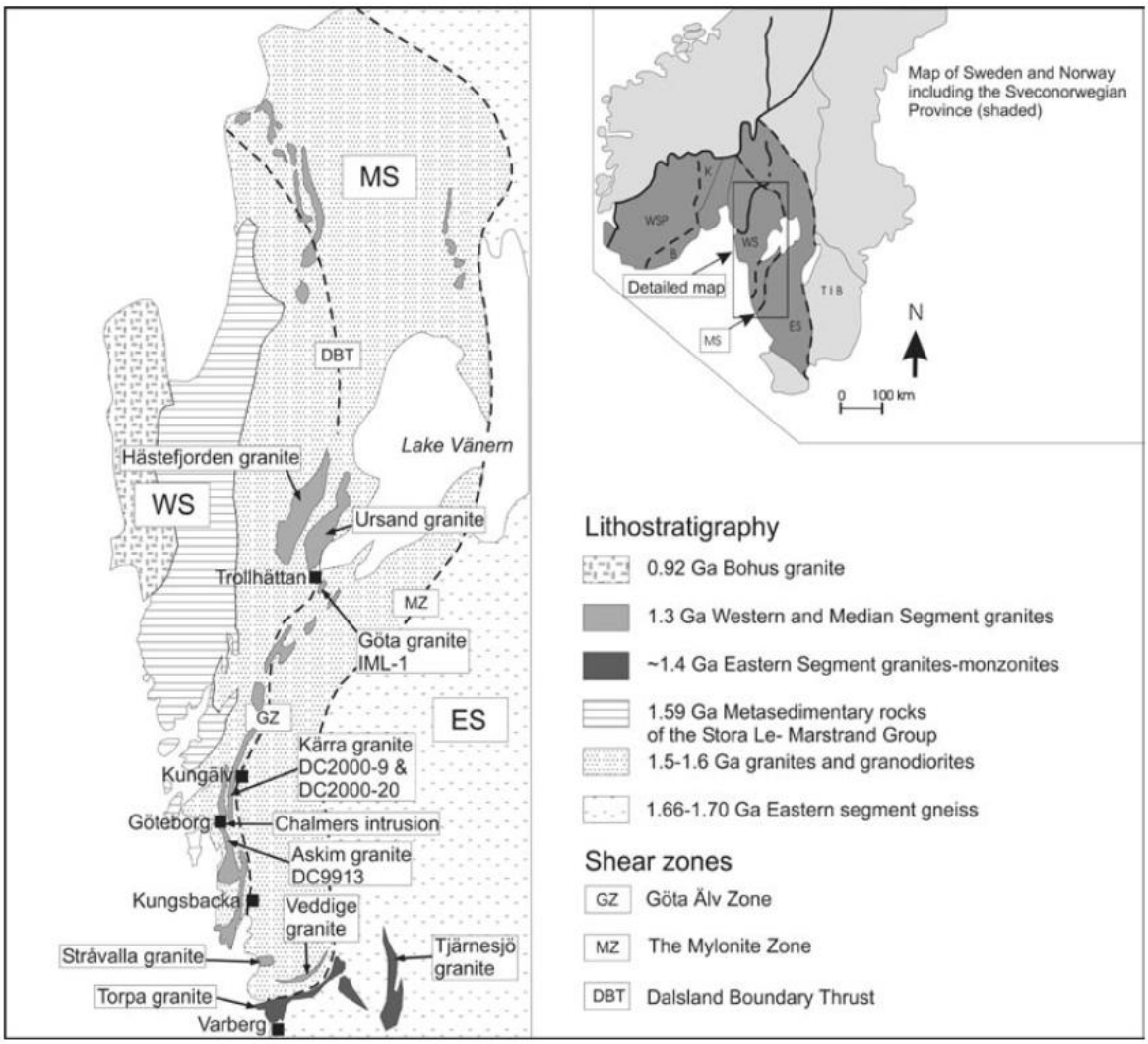

Figure 5: Geological map showing the location of the major rock units of the Swedish part of the Sweconorwegian province. WS - Western segment, MS - Median segment, ES - Eastern segment. Image from Hegardt (2007)

The subject of this study is a gabbroitic body which intruded the surrounding Askim granite shortly after the granite cooled, around 1336±10 Ma (Hegardt et al., 2007). The Askim granite is red-grey to grey, rich in 0,5-5 cm microcline augen, and often appears gneissic. The density of the granite is assumed to be 2,65 g/cm^3 and the density of the gabbro is assumed to be 3,0 g/cm^3, but they can vary slightly. (Lundqvist & Kero, 2006). This density difference makes them distinguishable by gravimetry. When the gabbro intruded, the granite partially melted on contact with the hot gabbro to create a plagioclase and quartz rich tonalite, which forms thin sheaths in the gabbro and granite. These tonalite sheaths are a good indicator that the contact between the two units is close (E. Sturkell, personal communication, 20 Apr 2023).

Recent previous research

The bedrock around the Billdal area has been extensively studied due to its interesting geology and proximity to Gothenburg. This has enabled earlier students to conduct their bachelor's, master's and PhD theses here. Projects like these have amassed data which are of paramount importance for this project. 924 outcrops have been mapped and classified and 395 gravity

measurements have been taken over the last decade (Fig. 4). The latest project to be conducted in this area (Tormos, 2021) attempted to estimate the volume of gabbro in the Billdal area. This was done by interpolating gravity measurements and attempting to model the bedrock in 3D and simulate two gravity profiles in the software ModelVision to match the interpolation. The resulting gabbro volume approximation was $4{,}10*10^8$ m^3. The following simulation assumed for simplicity's sake that the gabbro body is a large pluton, but Tormos emphasizes that the symmetry of the gabbro bodies are rough estimates that most likely do not correspond to how the bedrock actually looks. This results in a simulation which does not explain the sharpness of the positive gravity anomaly peak (Fig. 4). Nevertheless, Tormos data confirmed there is a 5,76 mGal gravity anomaly in the Billdal-Hällesås area.

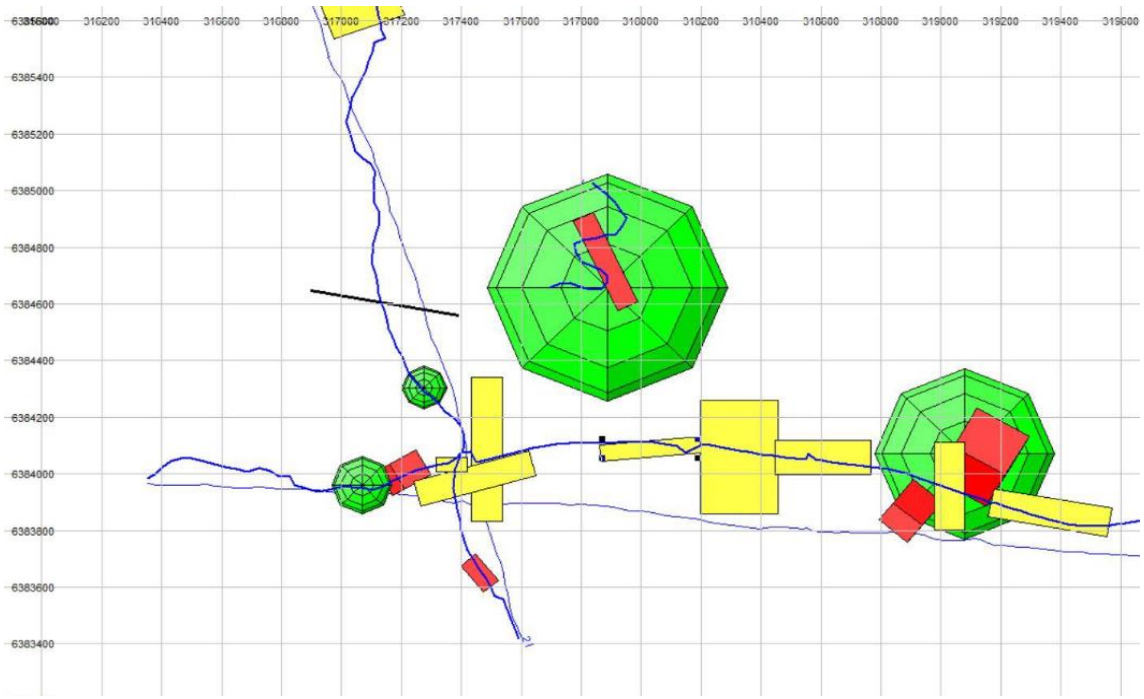

Figure 6: ModelVision rock bodies used to simulate the gravity anomaly interpolation by Tormos (2021). Yellow corresponds to clay of density 1600 kg/m^3, Red and green corresponds to gabbro of varying densities 2,95-3,20 g/cm^3

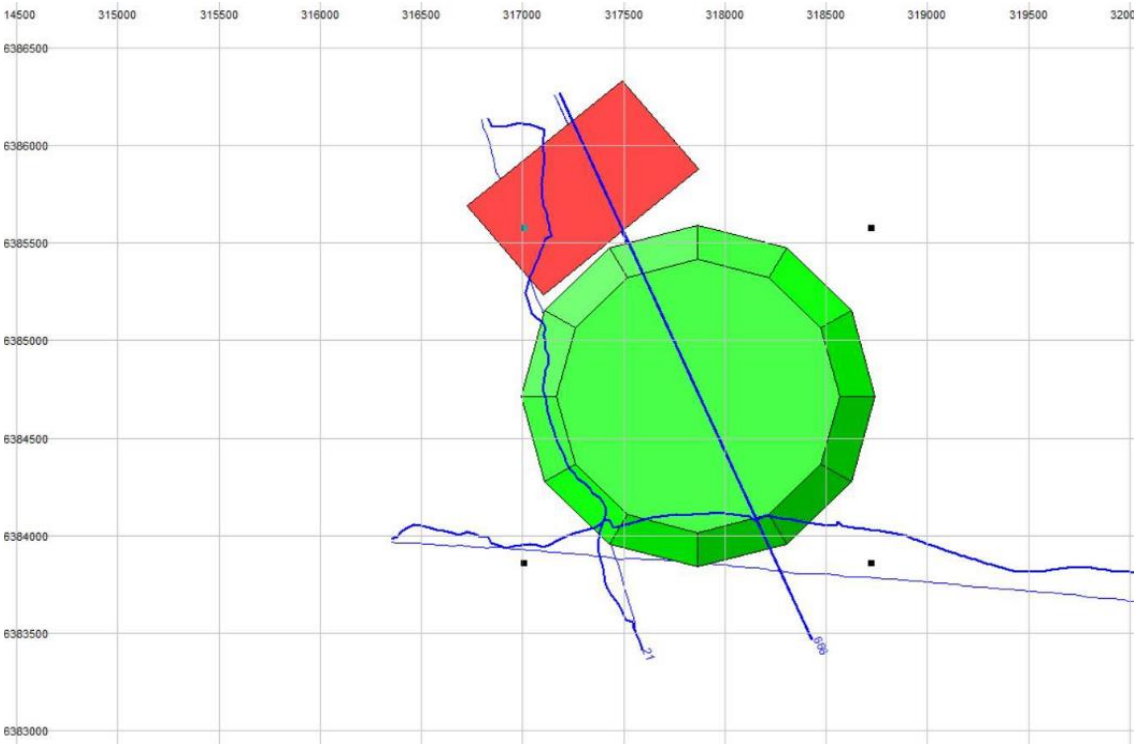

Figure 7: Alternative bodies used to simulate the gravity profile shown in the picture (the straight line) produced by Tormos (2021). Red is granite with the density 2,65 g/cm^3 and green is gabbro with an assumed density of 3,10 g/cm^3.

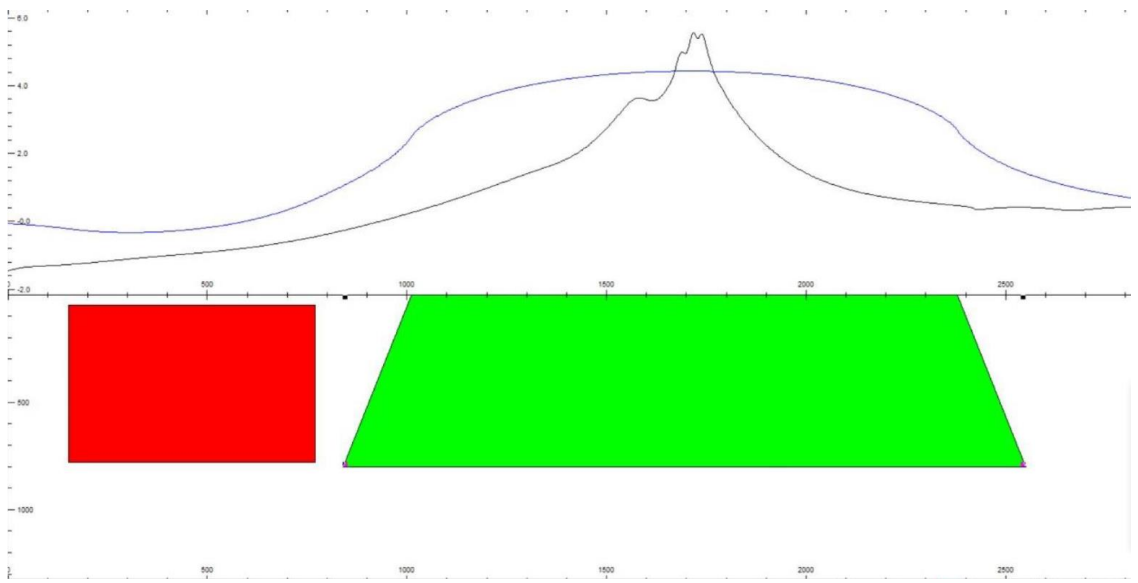

Figure 8: N-S simulated gravitational profile over the measured gravitational anomaly based on the shapes from figure 7. The fit of the simulated gravity (blue line with dull peak) to the interpolated gravity (black line with sharp peak) is not very close. (Tormos, 2021)

Hypothesis and aim

The Billdal bedrock map and gravitational anomaly map created by SGU is mismatched at first glance. A large positive gravitational anomaly would be expected where there is a gabbro body surrounded by granite. Despite this, the large gravitational anomaly lies roughly 1,5 km west of where the approximately 1,5 km^2 gabbro field is located (Fig. 2 and 3). The leading hypothesis of how the gabbro body is shaped is based on SGU's gravitational readings and bedrock map. The large positive gravitational anomaly (Fig. 3) is theorized to be a gabbro magma conduit extending to a great depth. The gabbro field is theorized to be a sill of gabbro originating from the magma conduit with a dip angle slightly higher than of the intersecting topography, creating a wide field of gabbro that can be easily mistaken for a massive gabbro body. Further supporting evidence lies in the fact that cracks filled with tonalite created from partial melting of granite can be found in the gabbro, signifying that the granite is close by in many places on the large gabbro field. This could mean that the gabbro field is fairly thin. attempt to model the bedrock over the whole study area to approximate the total gabbro volume, he lacked the data necessary to accurately model the large gabbro field. In contrast, this project is limited to just one profile over the Billdal–Hällesås area, allowing for greater focus on a smaller study area. (E. Sturkell, personal communication, 28 Apr 2023) Despite Tormos' (2021)

The aim of this study is to determine the shape and extent of the gabbro intrusion in the Billdal–Hällesås area.

Methods

The data used for the project was a combination of previously mapped outcrops, gravity measurements and new gravimetry data and outcrop mapping produced in this survey, collected in April 2023. The previously collected data consisted of 395 gravity measurements created during 2019-2022 (Appendix I) and 924 outcrops mapped during 2010-2022. This survey extended the datasets by 90 gravity measurements (Appendix II) to a total of 485 and 46 new outcrops to a total of 970.

Field measurements

The effect of altitude on gravity readings is much greater than the effect of bedrock density. To be able to nullify the effect altitude has on gravity, it is necessary to accurately know the height above sea level of the measuring sites. To accomplish this, a surveyor's levelling instrument with a spyglass and a tall folding rule was used to compare all measuring sites to fixed points with known heights (Fig. 9). This was done twice for each point to quickly identify any potential measuring errors and to achieve a ±1 mm accuracy. The measuring sites were recorded with a GPS and marked with spray painted before levelling.

Figure 9: Levelling tool in the foreground with a large folding rule in the background.

When levelling was done the raw gravity data could be read from a gravimeter (Fig. 10). A base point was regularly measured every 60-90 minutes to determine instrument drift and tidal drift. The raw gravity data required correction for several other parameters. All corrections were performed in Microsoft Excel. It was important for the measuring site to be reasonably flat and solid, as otherwise the gravimeter would take longer to stabilize and have a higher margin of error.

Figure 10: The LaCoste & Romberg gravimeter (model G-624) used in the survey. The green display where the readings are displayed is located in the bottom part of the gravimeter. This specific model has about the same shape and size as a car battery. Photo: E. Sturkell

Observations of rock type, strike, dip, and other notable outcrop characteristics were also noted with the corresponding GPS position.

Gravity corrections

The gravity corrections applied to the raw gravimetry data were instrument and tidal drift corrections, Bouguer correction, free air correction, latitude correction and terrain correction. These corrections were required to nullify factors which are larger than the effect of bedrock density on the gravitational field.

Drift correction

To correct for instrument drift and tidal effects over time, a base point was measured every 60 to 90 minutes. This allows for the magnitude of drift to be measured and compensated for. Best praxis is to start a measurement loop at the base point, take the measurements, and return to the base point. If more measuring loops are performed in a day the last base point measurement of the first loop acts as the first base point measurement for the second loop. Note that this approach only work with measurements collected in the same 24-hour day.

$$D_{\text{korr}} = ((B_1 - B_2)/T_1) * T_2 \quad (1)$$

Where:
Dkorr = Drift correction factor
B_1 = First base point reading (mGal)
B_2 = Second base point reading (mGal)
T_1 = Time difference between base point 1 and 2 readings (minutes)
T_2 = Time difference between base point 1 measuring point (minutes)

Some gravimeters give the gravity reading in scale units that must be manually multiplied with a scale constant that is unique for each individual gravimeter. This gives the reading in mGal. The gravimeter used for this study does this step automatically and can thus give the reading directly in mGal but the . This means that the scale constant S used in the equation for g_d (Eq. 2) in this case is equal to 1.

$$g_d = (P + D_{\text{korr}} - B_1) * S \quad (2)$$

Where:
g_d = Drift corrected g-value.
P = the measured value at the gravimeter survey point in question, in scale units Dkorr = Drift correction factor (from eq. 1)
B_1 = That day's first base point observation in scale units (or mGal).
S = The unique scale constant of the gravimeter.

Latitude correction

As Earth is a spinning ellipsoid rather than a stationary perfect sphere, the equator is slightly further from the planet's centre of gravity when compared to the poles. The spinning also creates a slight gradient of centrifugal force between the poles and the equator. The Earth's radius is 6378 km at the equator and 6357 km at the poles. The equation to account for both of these effects follows:

$$G_{teor} = G_{eq} * (1 + 0{,}005278895 * sin(\lambda)^2 + 0{,}000023462 * sin(\lambda)^4) \quad (3)$$

Where:
G_{teor} = Theoretical value for a specific latitude (mGal)
G_{eq} = 978031,841 mGal (The average gravity at the equator)
λ = Measurement site latitude (deg.)

Bouguer and free air correction

The Bouguer correction approximately compensates for the amount of rock between the height of the measuring point and the base point. This is done by applying an infinitely large plate with the density of the local bedrock, which fills up space between the height of the base station and the survey site (Fig. 11). This overcompensates by filling in the air as well, but this is corrected for by the terrain correction. The free air correction compensates for the lowering of gravity with higher altitude. The free air and bouguer corrections are most commonly used in the same equation:

$$G_{bf} = H * (0{,}3086 - 0{,}04191 * D) \quad (4)$$

Where
G_{bf} = Bouguer- free air correction factor
H = height difference between base point and measuring point (m)
D = Approximate average density of the local bedrock (g/cm^3)

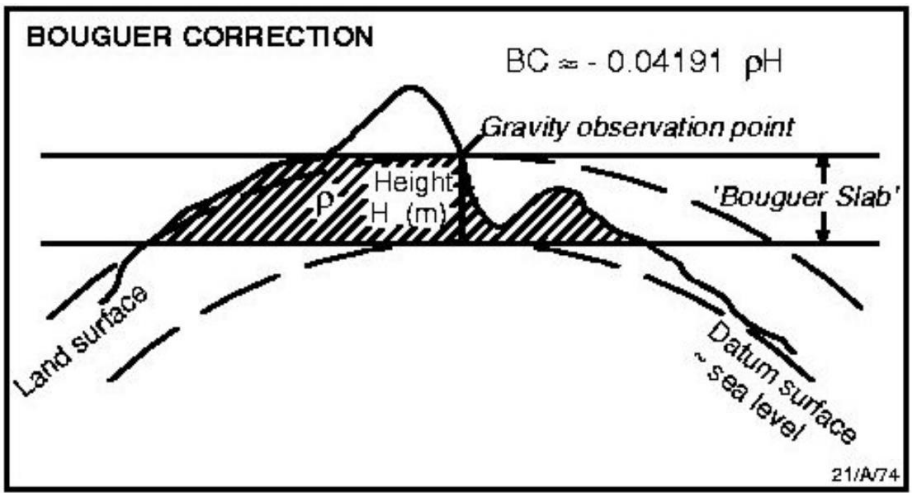

Figure 11: Diagram of the bouguer plate. Zhou, 2009

Terrain correction

When measuring the gravity immediately adjacent to a large cliff or a mountain, the mass that lies above the gravimeter contributes to a small but noticeable net-upwards gravitational pull. The terrain correction compensates for this extra upwards pull as well as for the air filled in by the infinite bouguer slab (Fig. 11). This correction is the most advanced to conduct and carries a lot of uncertainty in rugged terrain. The correction was performed in a C program created by Prof. E. Sturkell. The program uses the measurement site coordinates and a digital elevation model (DEM) with 2m resolution (Lantmäteriet, 2020) in ascii format as input and gives a terrain correction constant calculated out to hammer zone F (894,9 m) for each measure point. (Appendix III)

Modelling

Qgis (v3.26.) was used to interpolate the corrected gravity readings in order to create gravity anomaly profiles. ModelVision (v17.5.) was used to simulate the gravity response on the same gravity profile by building the bedrock from simple shapes with different densities. There are several reasons for not attempting to model gravity anomalies over the whole area. Firstly, Tormos (2021) already attempted this with mixed results regarding the structure of the gabbro body. Secondly, profiles are also more time efficient and require less work than simulating the whole area. An attempt to characterize the shape of the gabbro body in a geological profile based on outcrop observations was also made.

Table 1: The rock types and their densities used for modelling in ModelVision.

Rock type	Density (g/cm^3)
Granite	2,65
Gabbro 1	3,00
Gabbro 2	3,30
Clay	1,80

Results

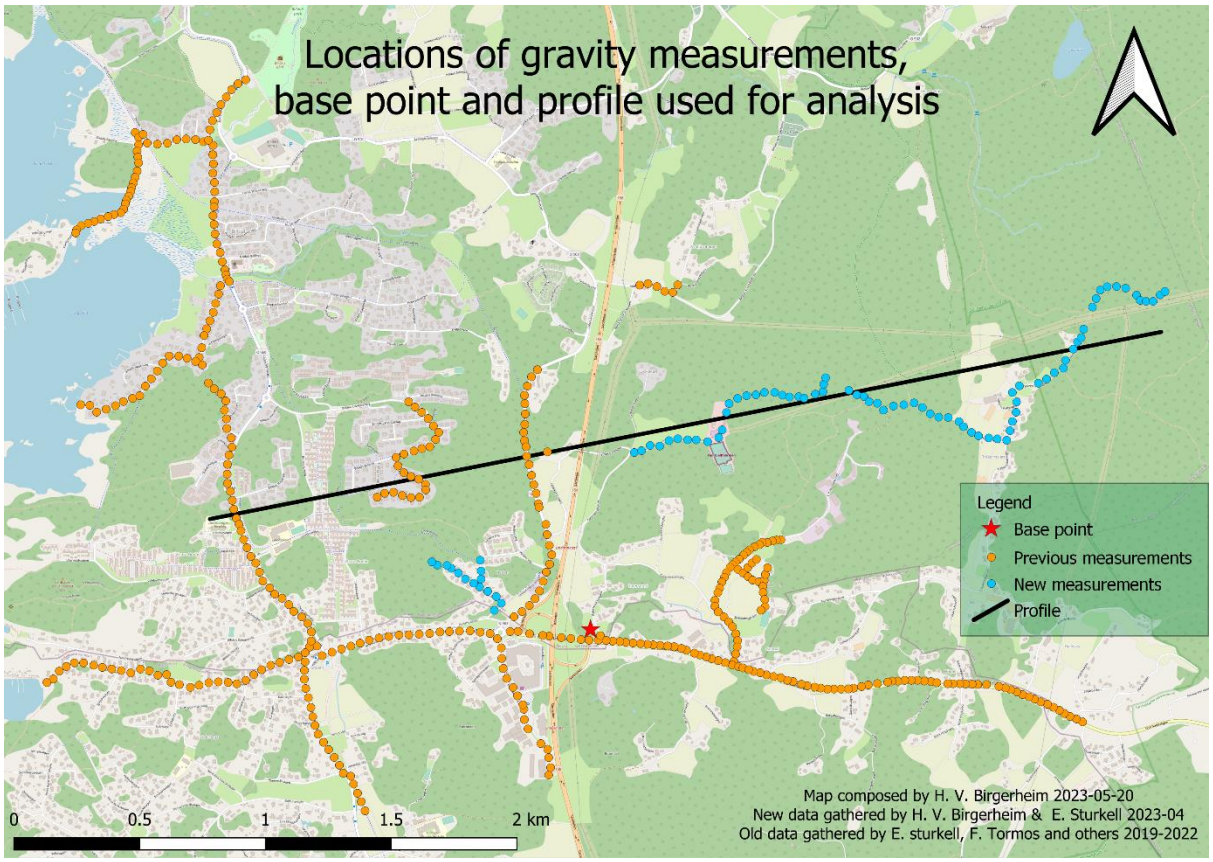

Figure 12: Gravity anomaly measurements from previous projects and the measurements taken for this specific project. Base point for all measurements is marked with a star. The profile used for analysis is marked in black.

The base point is close to and easily accessible from all the measurement sites (Fig. 12). It is also located on solid bedrock and away from disturbances larger than the sensitivity of the gravimeter. The profile is placed along the new measurements over the hypothesized sill to make the interpolation along the profile as accurate as possible. Measurements were taken on solid bedrock if available.

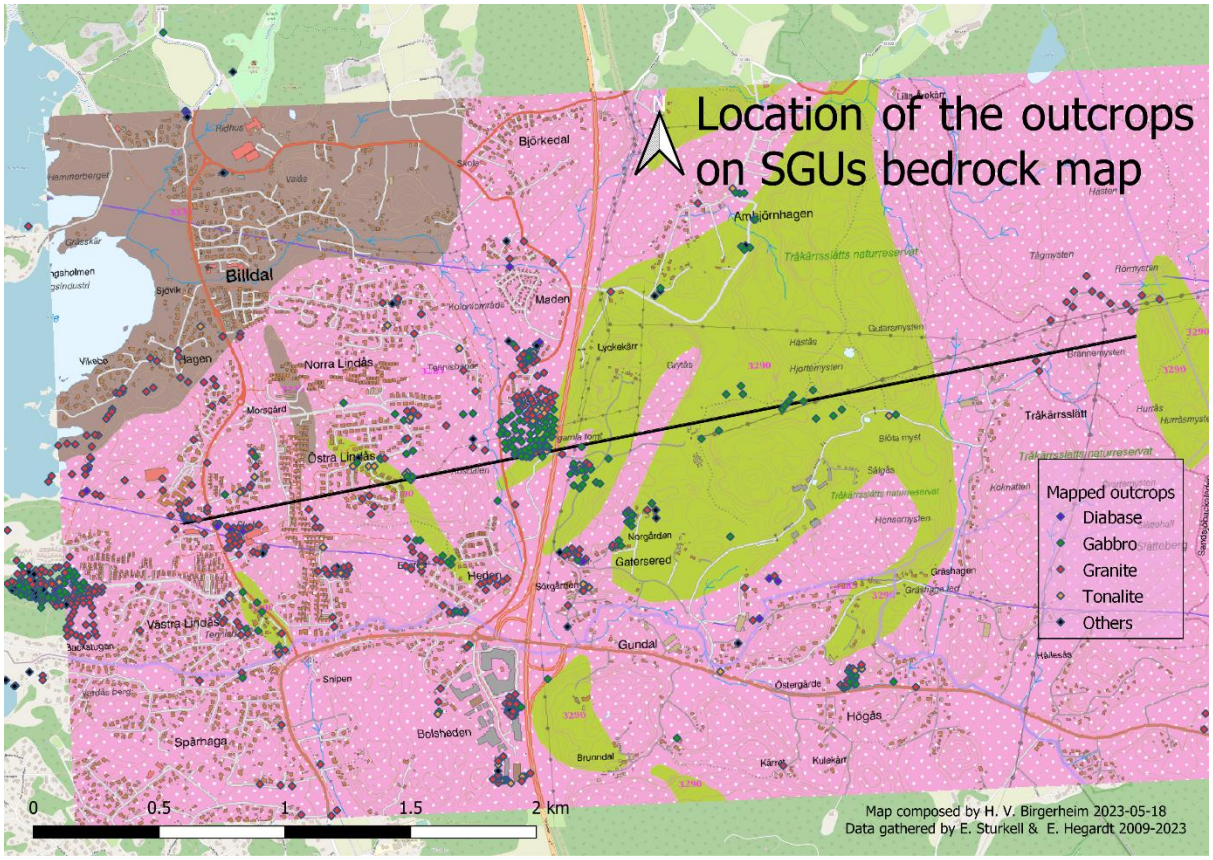

Figure 13: Mapped outcrops on top of the SGU bedrock map. Red is granite, green is gabbro, orange is tonalite, purple is diabase and black are others. The great majority of these outcrops were mapped during previous surveys and excursions.

The mapped outcrops largely agree with the bedrock map made by SGU. Although there are some granite outcrops in areas marked as gabbro by SGU and vice versa, the gabbro-granite contactsfound in the field are similar to the areas reported by SGU (Fig. 13).

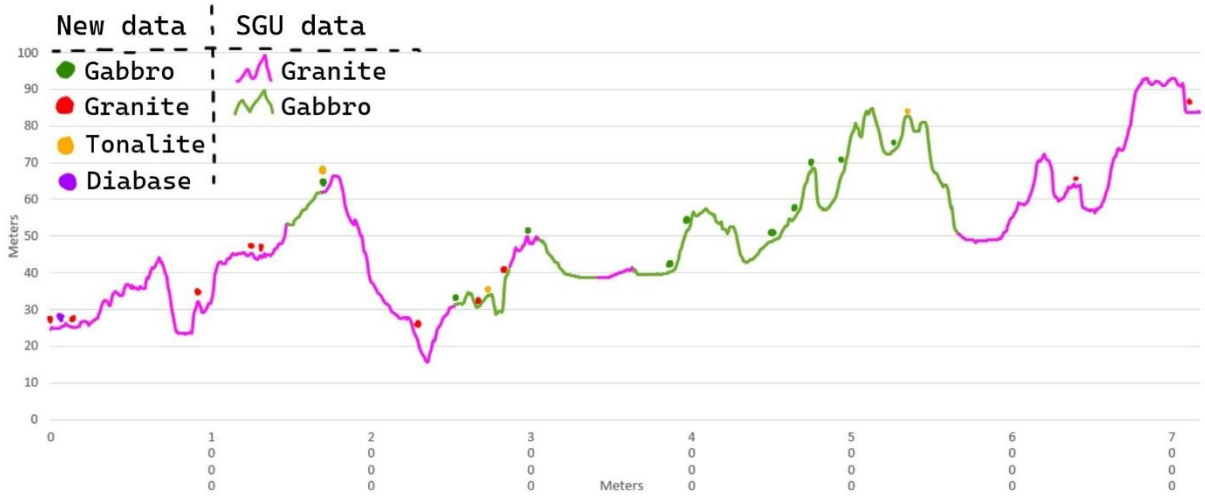

Figure 14: Graph of the altitude profile based on SGUs 2m digital elevation model. The colours represent what rock type is found where. Note that both axes are in meters and that the X axis is 23 times larger than the Y axis.

The mapped outcrops and the SGU bedrock map agree better along our profile compared the study area as a whole. This is by coincidence and could easily be skewed in the other direction by creating a profile somewhere else. The only outcrops which contest the SGU map lie in the 2500-3000 m section (Fig. 14). Some outcrops do not intersect perfectly with the profile and are taken from places up to ~50 m from the profile.

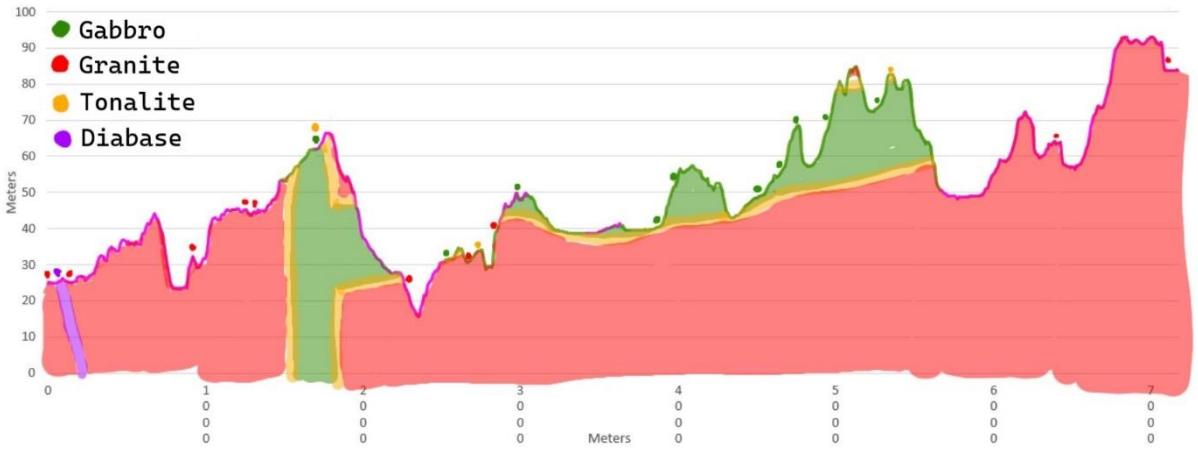

Figure 15: Digital illustration of how the bedrock could be structured based on the bedrock map from SGU and the measured outcrops. Sediments and joints are not included. Note that both X and Y are in meters.

Since SGU does not disclose which outcrops they base their maps on, our mapped outcrops were considered more accurate than the SGU map when sketching the bedrock structure (Fig. 15). A steep fault with a large normal component is a possible cause of why the gabbro cannot be found in the eastern segment of the profile.

Figure 16: Digital illustration of how the assumed gabbro magma conduit and sill could have looked before erosion. Note that both X and Y are in meters.

Although somewhat speculative, the bedrock above the current surface might have looked similar to figure 16 before erosion. The sill seems to be around 20-30 m thick. Based on a trigonometric calculation it shows an apparent dip angle of 0,79° towards the magma conduit, which might be the true dip assuming the profile intersects perfectly with the dip direction. The

sill geometry does not perfectly match either the mapped outcrops or SGUs bedrock map if assumed to be completely straight.

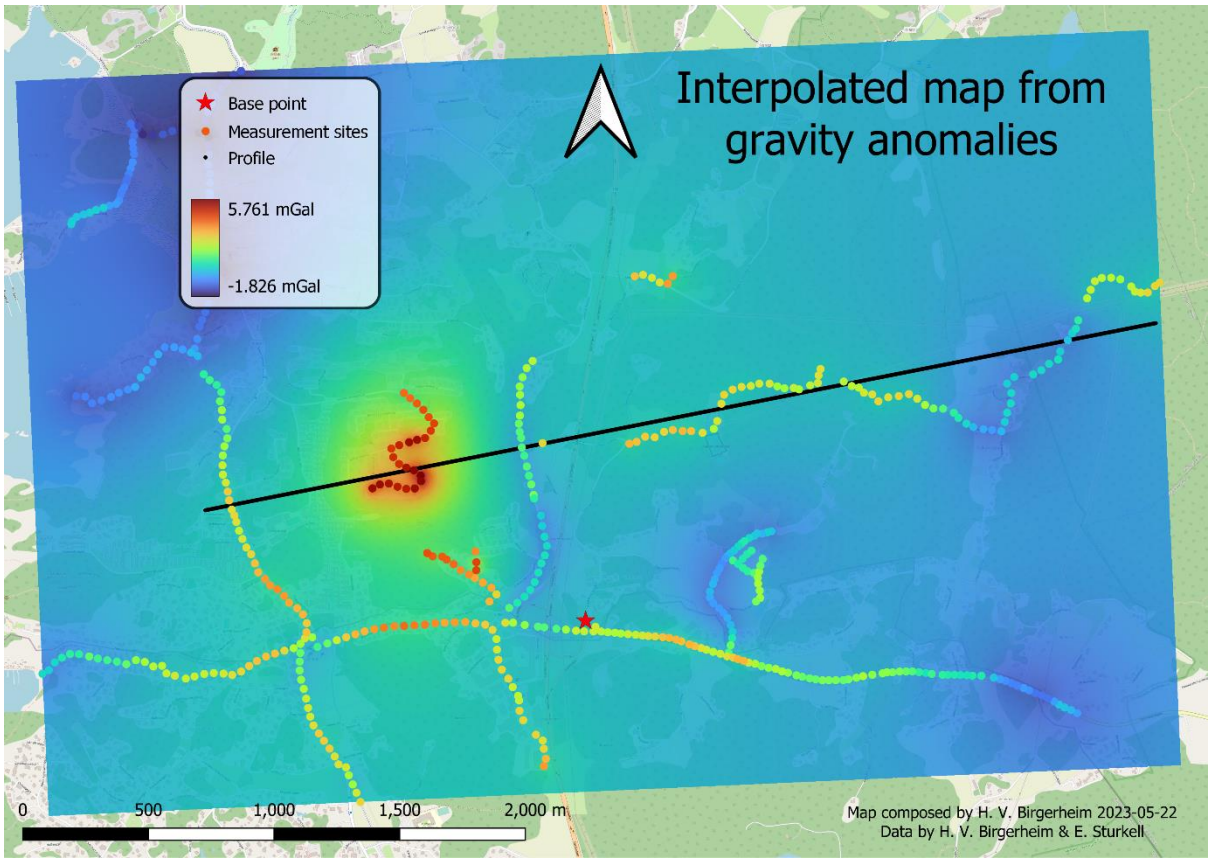

Figure 17: Map of all gravity measurements and an interpolated map of gravity anomalies.

The new interpolated map of gravity anomalies (Fig. 17) shows similarities with the gravity anomaly map created by SGU (Fig. 3). The high positive anomaly in the new map corresponds to where SGU placed their positive anomaly. The diameter of the anomaly appears to be detectable ~500 m from the anomaly peak. The base point itself is inside the area gravitationally affected by the gabbro. Since all gravity readings are relative to the base point, the values of both the gravity readings and the interpolation are positively skewed. The dark blue area in the north-west would be a more representative "normal" reading for the wider area. The colours of the points are slightly exaggerated to better show smaller variations in the data while the colour scale for the interpolation is linear.

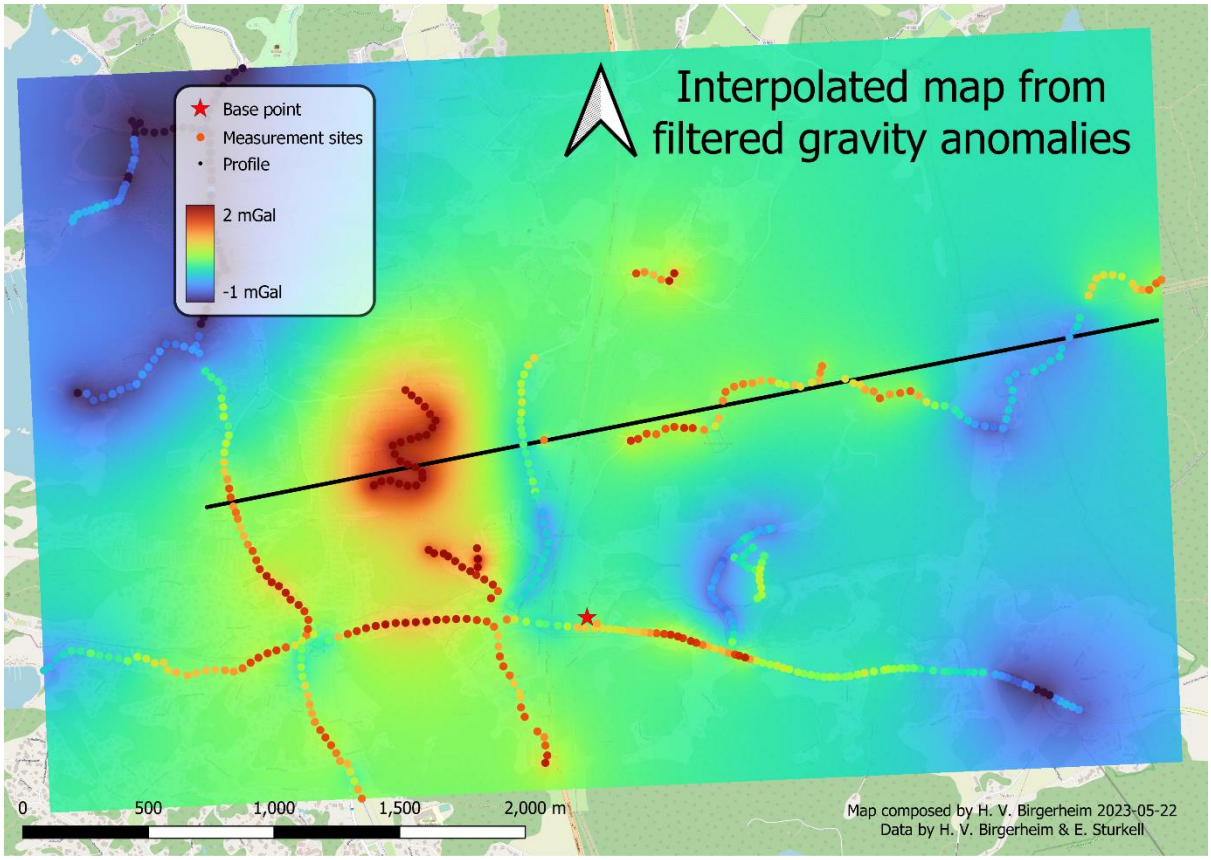

Figure 18: Interpolation of filtered gravity measurements where all values <(-1) are set to (-1) and all values >2 are set to 2.

Discarding the most extreme positive and negative values in the input data for the interpolation greatly improves the ability to distinguish between smaller variations in the values from (-1) – 2 mGal (Fig. 18). Furthermore, it can be observed that the plateau of slightly higher gravity readings shown by SGU (Fig. 3) around the large anomaly is of roughly the same shape as in the filtered interpolation.

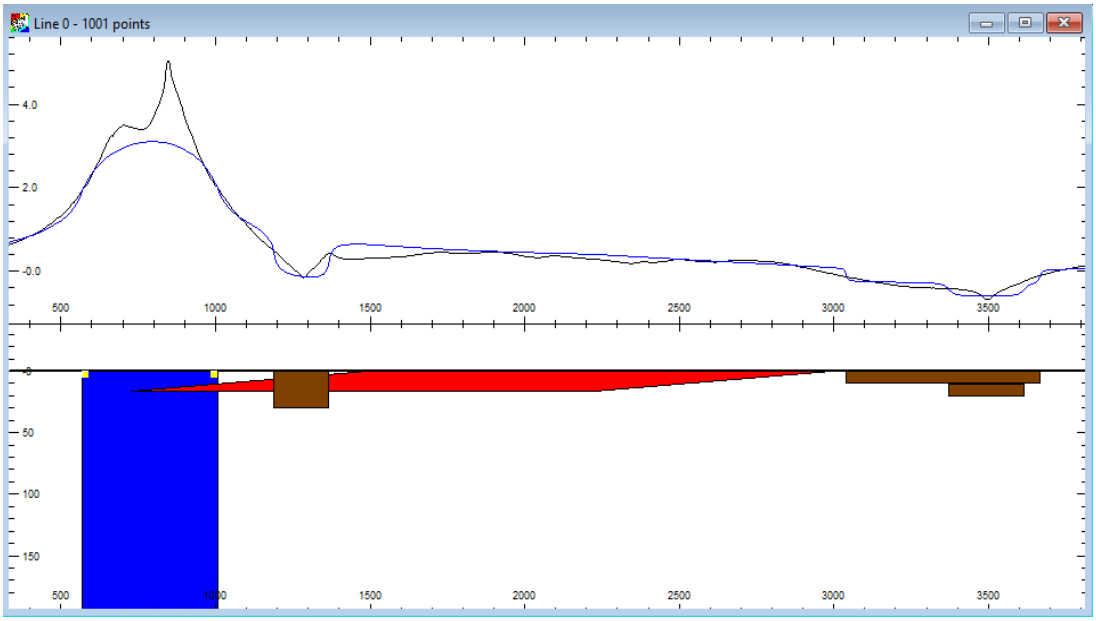

Figure 19: Gravity model (blue line) attempting to mimic the actual gravity readings (black line). The simple shapes represent the proposed bedrock structure. The white represents granite with the density 2,65 g/cm^3, the blue and red represents gabbro with the density 3,00 g/cm^3 and the brown represents fracture valleys filled with marine clay, with the density 1,80 g/cm^3.

The gravity simulation of the hypothesized bedrock structure lines up very well with the gravity anomaly profile of the interpolation from the measured gravity anomalies, except for the peak (Fig. 19). The gabbro magma conduit in blue has the diameter 220 m and goes down to a depth of 5000 m.

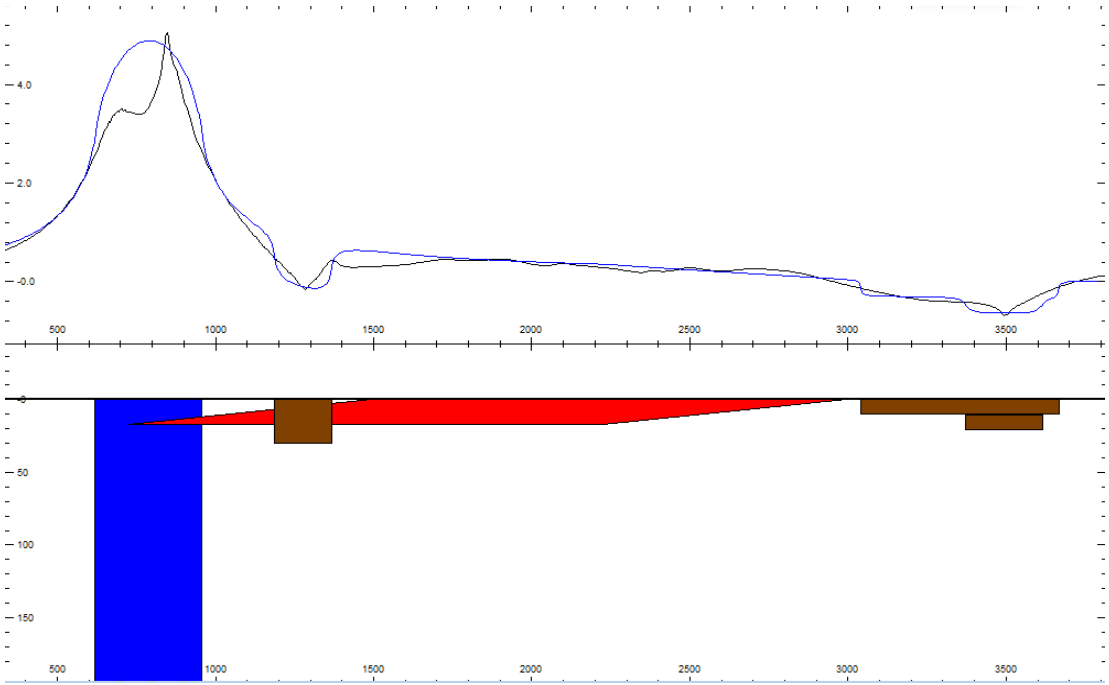

Figure 20: The same gravity model as in figure 12, but with a thinner gabbro magma conduit (blue rectangle) with the density 3300 kg/m3. No other parameter has been changed.

The only way for the simulated profile to approach the interpolated profile was to raise the density of the gabbro magma conduit to that of the upper limit of gabbro and to lower the diameter to 170 m and the depth to 2000 m (Fig. 20).

Discussion

Results summary

The values of the positive gravity anomaly peak are much higher than the rest of the interpolation (Fig. 17). This decreases the range of the colour gradient, making smaller details in the data hard to see. This was solved by filtering the measured gravity by limiting the peaks and troughs to 2 and (-1) mGal respectively (Fig. 18). This effectively stretched out the colour gradient to emphasize the finer details for values ranging from (-1) to 2. Similarities with the gravity interpolation and SGU's gravity anomaly map are visible (Fig. 18 & 3), with a large peak and a shelf of slightly elevated gravity where the gabbro field is located (Fig. 2). Joint valleys are clearly visible on the eastern and western side of the gabbro field in the interpolated gravity map by their negative anomalies.
The geological profile based on elevation and observed outcrops (Fig. 15) suggest that the sill is around 20-30 m thick with a 0,79° apparent dip angle towards the suggested gabbro magma conduit. The sill cannot be assumed to have a constant dip angle based on the outcrops along the profile. Although the geological profile fits with the magma conduit and sill hypothesis, it could still be greatly improved with more mapped outcrops along the profile. A steep normal fault is believed to cut of the gabbro sill in the eastern part of the geological profile.
The gravity simulation in ModelVision (Fig. 19) agrees with the interpolated gravity readings well, apart from the large peak where the gabbro magma conduit is hypothesized to be. This peak proved unattainable with a gabbro tube of any dimensions with the density 3,00 g/cm^3. When the gabbro magma conduit was made smaller and its density was raised to 3,30 g/cm^3, the simulated gravity peak fit the interpolated gravity peak much more closely (Fig. 20).

Comparison with previous results

SGU's gravity anomaly map

The new interpolation (Fig. 16) made for this project and the gravity anomaly map by SGU (Fig. 3) are produced in significantly different ways and cannot be held to the same standards. The Swedish Geological Survey (SGU) compiles a gravity anomaly map covering all of Sweden and the latest version is from February 2020. The measurements originate from several sources: SGU themselves, Lantmäteriet, universities, as well as private and public companies. Some of the measurements are made in collaboration with Finland and Denmark. The density of measurements varies significantly depending on location. Mining areas usually have dense coverage and remote areas such as the Scandes mountain range usually have very low measurement density if any. SGU does not disclose exactly where each measurement is taken, what value each reading has or their margin of error (SGU, 2020).

The interpolation made for this study is based on ground measurements which are tightly packed in some areas but absent in others. This produces a map with varying accuracy depending on geographical closeness to the measuring points. Our gravity anomaly interpolation confirms the gravity anomaly above the supposed magma conduit in SGU's gravity anomaly map, and adds a great deal of new detail. The interpolation also confirms the slight positive anomaly over the large gabbro field to the east of the anomaly peak that is hinted at in SGU's gravity anomaly map. This result is in line with what would be expected if the gabbro would be a thin layer and not a massive body.

SGU's bedrock map

The measured outcrops largely agree with the SGU bedrock map. With that said, it is by no means a perfect match. There are several outcrops that do not agree with the SGU interpretation of the bedrock, especially in between the large gabbro field (Fig. 2) and the large gravity anomaly (Fig. 3). There is believed to be a very steep fault in the eastern part of the profile. This could explain both the lack of gabbro in the eastern part of the profile as well as the placement of the eastern clay filled valley (Fig. 18). The geological profile is based on the measured outcrops because SGU does not publish which outcrops they base their bedrock map on. It is very probable that SGU used far fewer outcrops than this study has access to, and that these could be used to more accurately map the area we are interested in.

Tormos (2021)

Tormos (2021) estimation of the shape of the gabbro body that causes the large positive gravitational anomaly differs quite a bit from this study, and he mentions similar problems with matching the simulated peak with the interpolated peak. There are a few reasons for why his simulation does not match the anomaly peak. His aim was to estimate the volume of mafic rock in the area, not to necessarily figure out its geometry. He used two different shapes to estimate the gabbro body, a large sphere and a large cone with a blunt top (Fig. 7 & 8). Both were mentioned to be approximations that did not necessarily correspond to the real bedrock structure. Tormos also stated that the density of the gabbro could be higher. When he experimentally raised the density of the gabbro in ModelVision, it fit better with the interpolated gravity. This project experienced the same problem with matching the simulated gravity peak, which could be solved by raising the density of the magma conduit from 3000 kg/m3 to 3300 kg/m3.

Tormos also modelled a second gabbro sphere to the south-east of the large positive anomaly peak (Fig. 6). The gravity interpolation made for this study (Fig. 16 & 17) does show a slightly heightened gravity in this spot, but it is not nearly as large as the prominent gravity anomaly west of road 158. The additional gabbro sphere appears more similar to the proposed sill east of road 158 than with the proposed magma conduit.

Interpretations

Except for the magma conduit, the modelled gravity profile with the 3000 kg/m3 density (Fig. 18) fits in very well with the gravity profile from the interpolated gravity measurements when adding basic shapes which resemble the theorized shape of the gabbro body. A deep magma conduit and a sheet extending eastward is a highly probable cause of why the large positive gravity anomaly is located where it is, and why the large gabbro field only causes a small positive gravity anomaly. The negative gravity anomalies are believed to originate from fracture valleys filled with a layer of marine clay. These dips in the gravity anomaly profile could not be accurately simulated by only adding bodies of higher densities than the background density of 2650 kg/m3. Bodies of lower densities representing the clay with 1800 kg/m3 can accurately imitate the interpolated gravity anomaly profile.

An interesting realization, which was also theorized by Tormos (2021), is that the simulated gravity fits much better if the density of the gabbro is higher. One potential way for this to be explained is if the last magma to pass through the magma conduit is the mafic mush that fractionally crystallizes and slowly settles to the bottom of the magma chamber. This would result in the centre of the magma tube to contain heavier minerals than the rest of the gabbro, thus giving a stronger local gravitational reading. Magma conduits are known to be reused and can erupt several times during periods of repeated volcanism. This happens because they are the last to cool down and solidify, making them the weak point in the crust that magma can penetrate through. (E. Sturkell, personal communication, 17 May 2023)

Furthermore, such a magma conduit with a denser central part has been observed in the Tösse area in the northern part of the Kungsbacka bimodal suite (E. Hegardt, personal communication, 16 May 2023), making this new hypothesis a possible explanation as to why the large gravitational anomaly stands out so much compared to the surrounding.

Despite its large area, the gabbro field does not show any gravitational signs of extending very far down. This seemingly eliminates theories of the field being a massive body. However, this is only certain to be true along our profile. Since the large gravitational anomaly in the interpolation produced for this study have a detectability radius of ~500 m, there could theoretically be a similar magma conduit ~500 m from the profile without leaving a trace. However, this is unlikely based on the gravity map compiled by SGU.

The simulated gravity profile alone is not conclusive proof of our hypothesis since wildly different geometries of rock bodies can give almost the exact same gravitational profile (Pitney Bowes Software Inc., 2012). It is when different methods indicate the same thing that the credibility of a theory increases dramatically. When both the gravity model and the bedrock profile indicate that the hypothesis is possible, it becomes more likely than if only one of these methods would be used alone.

A north-south striking normal fault in the eastern part of the profile (Fig. 15) is a possible explanation for why the gabbro is not found in the east. The exact parameters of the fault are unknown, but some things can be assumed. Firstly, it can be assumed to not be a transverse fault. This would be easily spotted in the diabase dyke that crosses the fault south of the gabbro field in the geological map by SGU (Fig. 12). Secondly, it can also be assumed that the eastern

part of the fault rose in relation to the western part. If the opposite would be true the gabbro sill would still exist underground east of the fault, which would probably be detected by the gravimeter if not buried exceedingly deep.

Uncertainties and further research

There are a few uncertainties regarding the data that was gathered from the survey. The first is that the gravimeter has an innate uncertainty of 0.01 mGal. This uncertainty varied slightly depending on the ground surface, but it was usually lower than this, which was indicated by the gravimeter by displaying the final value quickly. The levelling aimed for an uncertainty less than 2 mm and achieved an uncertainty of ~1 mm. Latitude was measured by handheld GPS with an accuracy of ±3 m, but it might be slightly lower than this for some measurements. Lastly, the 2m DEM from Lantmäteriet used for terrain correction has an uncertainty of 0,105-0,593 m depending on the degree of sloping and vegetation type (Mörtberg & Kulla, 2012). Even combined, these uncertainties are small and are not expected to have had any significant effect on the outcome of this project.

Based on the geological profile (Fig. 15) this study theorizes that the gabbro sill has a thickness of around 20 – 30 m. To know the thickness of the sill and to learn more about the normal fault, drill cores from the area should be produced and examined. This is the only way to be fully certain of the subsurface. Drawbacks with this are that parts of the terrain is very rough for a drill rig and that it is more expensive than geophysical methods.

This project likely uses more outcrops than SGU had access to when creating their bedrock map (Fig. 12). An updated bedrock map could be created based on the outcrops used for this project. This would enable more accurate geological profiles to be created in the area.

Lastly, to ensure what density should be used to model the gravity anomaly in ModelVision, a thorough density investigation could be conducted on gabbro outcrops on the large anomaly. Even better would be to do this from core samples taken from different parts of the magma conduit, to make sure that different densities depending on closeness to the centre will be detected if they exist.

Conclusions

The aim of this study was to determine the shape and extent of the gabbro intrusion in the Billdal–Hällesås area.

- The large gravity anomaly is likely caused by a deep gabbroitic magma conduit based on gravity anomaly data and shown by a simulated gravity profile.
- Assumed net density of the magma conduit is likely higher than the assumed 3 g/cm^3 since the simulated gravity anomaly peak fit better with a magma conduit density of 3,3 g/cm^3.
- The gabbro field east of road 158 shows no gravitational sign of being a massive body.
- Geological profiling indicates that the gabbro field is likely to be a 20 – 30 m thick sill with an average dip angle of at least 0,79° towards the magma conduit to which it is connected.
- The sill is likely terminated to the east by a steep north-south striking normal fault.

References

Austin, H. E., Cornell, D. H,. Hellström, F. A., Lundqvist, I. (2007). Emplacement ages of the mid-proterozoic Kungsbacka bimodal suite, SW Sweden. *Taylor & Francis Online, 129*(3), 227-234, DOI: 10.1080/11035890701293227

Berthelsen, A., 1980: *Towards a palinspastic tectonic analysis of the Baltic Shield.* J. Cogné & M. Slansky (eds.): Géologie de l'europé du Précambrien aux Bassins sédimentaires post-hersyniens, 5–21. Congrés Géologique International. Colloque C6. Paris.

Bingen, B., Nordgulen, Ø. & Viola, G. (2008). *A four-phase model for the Sweconorwegian orogeny*, SW Scandinavia. Norwegian Journal of Geology vol. 88, pp 43–72.

Lundegårdh, P. H., & Sandegren, R. (1953). *Beskrivning till kartbladet Särö*. Norstedt & Söner

Lundqvist, I., Kero, L. (2006). *Beskrivning till berggrundskartan 7B Göteborg SV*. Sveriges Geologiska undersökning. https://resource.sgu.se/dokument/publikation/k/k60beskrivning/k60-beskrivning.pdf

Mörtberg, M., Kulla, H (2012). *Vegetation och lutningars påverkan på osäkerheten hos laserdata för en ny nationell höjdmodell* [Bachelor thesis, Högskolan i Gävle]. DiVA. https://hig.diva-portal.org/smash/record.jsf?pid=diva2%3A533301&dswid=8759

Pitney Bowes Software Inc. (2012). *Encom ModelVision™ v12.0 Geophysical Interpreters Guide*. https://manualzz.com/doc/24294311/encom-modelvision-v12.0.

SGU. (2023). *Kartvisaren Berggrund 1:50000-1:250000*. https://apps.sgu.se/kartvisare/kartvisare-berg-50-250-tusen.html. Accessed: 2023-05-15.

SGU. (2023). *Kartvisaren Tyngdkraft*. https://apps.sgu.se/kartvisare/kartvisare-tyngdkraft.html. Accessed: 2023-05-15.

SGU. (2020). *Tyngdkraft*. SGU. https://www.sgu.se/om-sgu/verksamhet/kartlaggning/geofysik_att_se_ner_i_berget/tyngdkraft/

Sturkell, E., Hegardt, E. (2020). *Regional Geology in the Gothenburg area*. [Unpublished report]. Geoscience department, University of Gothenburg.

Tormos, F. E. (2021). *Gravity survey of mafic rocks at Billdal* [Bachelor thesis, Göteborgs universitet]. Gothenburg university publications Electronic Archive. https://gupea.ub.gu.se/handle/2077/69076

Vladimirov, A. G., Izokh, A. E., Polyakov, G. V., Babin, G. A., Mekhonoshin, A. S., Kruk, N. N., Khlestov, V. V., Khromykh, S. V., Travin, A. V., Yudin, D. S., Shelepaev, R. A., Karmysheva, I. V., Mikheev, E. I. (2013). Gabbro-Granite intrusive series and their indicator importance for geodynamic reconstructions. *Petrology, 20(2),* 158-180. DOI: 10.1134/S0869591113020070

Zhou, X. (2009). 3D vector gravity potential and line integrals for the gravity anomaly of a rectangular prism with 3D variable density contrast. *Geophysics 74*(6). DOI:10.1190/1.3239518

Åhäll, K., Connelly, J. N. (2007), Long-term convergence along SW Fennoscandia: 330m.y. of proterozoic crustal growth. *Precambrian research, 161(2008),* 452-474, doi:10.1016/j.precamres.2007.09.007

Appendix I

Table with point ID, gravimeter reading, coordinates in SWEREF99, altitude, latitude, terrain correction constant and corrected gravity value. This is the data produced during previous projects.

			Instrument constant=	**1**		**density=**	**2,67**	
	BASE POINT							
	Reading	Time (h,min)	X-coordinate	Y-coordinate	Altitude (m)	Latitude (deg)		
Bas 1	1,512	13,54			39,424	57,56291315		
Bas 2	1,545	15,29						
Point	Reading	Time (h,min)	X-coordinate	Y-coordinate	Altitude (m)	Latitude (deg)	Terrain B-F	Dg (teor)
19GB035f	6,781	14,06	316800,1186	6386145,11	11,988	57,57496667	0,045569	-1,075768155
19GB036	6,853	14,1	316813,1794	6386125,38	11,662	57,57486667	0,041537	-1,065105506
19GB037	6,845	14,12	316811,2348	6386095,52	11,561	57,5747	0,039855	-1,081668244
19GB038	6,897	14,14	316803,9028	6386070,84	11,648	57,57455	0,084166	-0,956626367
19GB039	6,81	14,7	316805,6373	6386047,11	11,8385	57,57445	0,144205	-0,957360116
19GB040	6,708	14,19	316808,0813	6386023,78	12,0245	57,57431667	0,149324	-0,988994416
19GB041	6,817	14,22	316801,38	6385992,01	11,706	57,57415	0,193091	-0,886237716
19GB042	6,888	14,24	316792,156	6385968,2	11,397	57,57401667	0,127691	-0,931168137
19GB043	6,912	14,26	316784,0357	6385945,96	11,225	57,5739	0,069651	-0,990158687
19GB044	6,862	14,28	316775,8216	6385926,84	11,343	57,57378333	0,032275	-1,045442131
19GB045	6,88	14,3	316771,6469	6385912,65	11,3455	57,57378333	0,023806	-1,036114117
19GB046	6,912	14,32	316762,8583	6385894,43	11,3375	57,5736	0,021177	-0,993962387
19GB047	6,92	14,34	316753,4826	6385877,79	11,3465	57,57351667	0,032893	-0,966330321
19GB049	6,958	14,36	316748,4911	6385864,08	11,2415	57,57343333	0,027134	-0,948597079
19GB050	6,976	14,38	316739,6263	6385842,85	11,4045	57,57331667	0,017498	-0,899288938
19GB051	7,025	14,41	316727,9819	6385830,47	11,3205	57,57325	0,019725	-0,860154443
19GB052	7,058	14,46	316700,8223	6385823,73	11,258	57,5732	0,015593	-0,841212731
19GB053	7,212	14,51	316677,0874	6385817,36	11,634	57,57316667	0,011129	-0,616718043
19GB054	7,244	14,55	316647,449	6385809,38	11,746	57,57311667	0,009643	-0,561458755
19GB055	7,219	14,57	316621,0383	6385800,19	11,611	57,57306667	0,014533	-0,604713701
19GB056	7,186	14,59	316597,2687	6385793,81	11,432	57,57303333	0,020037	-0,665377569
19GB057	7,214	15,01	316569,0053	6385786	11,372	57,57298333	0,00957	-0,656236986
19GB058	7,242	15,04	316550,1261	6385769,82	11,428	57,57288333	0,014739	-0,60488619

19GB059f	7,384	15,15	316546,0511	6385757,85	10,663	57,57281667	0,011681	-0,614768509
			Instrument constant=	1		density=	2,67	
	BASE POINT							
	Reading	Time (h,min)	X-coordinate	Y-coordinate	Altitude (m)	Latitude (deg)		
Bas 1	2,525	7,43			39,424	57,56291315		
Bas 2	2,463	9,25						
Point	Reading	Time (h,min)	X-coordinate	Y-coordinate	Altitude (m)	Latitude (deg)	Terrain B-F	Dg (teor)
19GB079	-1,508	7,55	320424,7704	6383641,57	52,5885	57,5557	n.a.	
19GB080	-1,677	7,59	320457,6064	6383643,31	53,0865	57,5557	0,079822	-0,832798939
19GB081	-1,504	8,03	320434,398	6383655,88	52,7655	57,55576667	0,075704	-0,730100348
19GB082	-1,392	8,05	320409,0879	6383667,48	52,6105	57,55583333	0,078288	-0,650263186
19GB083	-1,388	8,08	320386,7311	6383679,97	52,2965	57,5559	0,120881	-0,669084523
19GB084	-1,438	8,11	320367,7311	6383693,29	51,8455	57,55596667	0,07363	-0,858697796
19GB085	-1,561	8,14	320345,1047	6383705,51	51,6015	57,55601667	0,07029	-1,035314611
19GB086	-1,597	8,17	320321,6898	6383718,52	51,5345	57,55608333	0,070335	-1,088098958
19GB087	-1,531	8,2	320294,5696	6383730,34	51,346	57,55613333	0,070833	-1,060960898
19GB088	-1,402	8,23	320271,2335	6383742,41	51,501	57,5562	0,080859	-0,895096768
19GB089	-1,371	8,26	320249,3954	6383752,42	51,5485	57,55625	0,073132	-0,86476243
19GB090	-1,474	8,31	320224,0096	6383762,43	51,4405	57,5563	0,067693	-0,995511299
19GB091	-1,418	8,33	320201,7773	6383773,39	51,2525	57,55635	0,079052	-0,968021718
19GB092	-1,414	8,36	320178,6619	6383782,58	51,5225	57,5564	0,090027	-0,902219553
19GB093	-1,422	8,4	320157,3522	6383790,58	51,8845	57,55643333	0,098433	-0,830913634
19GB094	-1,279	8,42	320132,124	6383797,95	51,9805	57,55646667	0,110296	-0,658688679
19GB071	-1,167	8,49	320082,535	6383807,92	52,251	57,55651667	0,274577	-0,329050784
19GB072	-1,145	8,51	320048,3982	6383809,93	52,42	57,55651667	0,219583	-0,327586747
19GB072b	-1,141	8,55	320026,1265	6383811,55	52,297	57,55651667	0,148243	-0,416689511
19GB073	-1,09	8,58	319999,6764	6383813,52	52,1265	57,55651667	0,111271	-0,434375383
19GB074	-0,972	9,02	319976,9316	6383816,32	51,9445	57,55653333	0,100046	-0,362336943
19GB075	-0,907	9,04	319949,8114	6383817,34	51,626	57,55653333	0,112731	-0,346085303
19GB076	-0,825	9,06	319929,3135	6383818,13	51,4095	57,55653333	0,140117	-0,278069231
19GB077	-0,658	9,1	319863,3262	6383828,54	49,8005	57,55656667	0,113288	-0,454694597
19GB096	-0,523	9,12	319886,2811	6383824,43	50,407	57,55655	0,129576	-0,181523701
19GB097	-0,354	9,14	319835,8118	6383832,95	49,1295	57,55658333	0,158659	-0,236246604

19GB098	-0,143	9,16	319809,8741	6383836,97	48,3975	57,5566	0,212113	-0,115930014

			Instrument constant=	1		density=	2,67	

BASE POINT

	Reading	Time (h,min)	X-coordinate	Y-coordinate	Altitude (m)	Latitude (deg)		
Bas 1	2,351	11,03			39,424	57,56291315		
Bas 2	2,336	12,41						

Point	Reading	Time (h,min)	X-coordinate	Y-coordinate	Altitude (m)	Latitude (deg)	Terrain B-F	Dg (teor)
19GB099	-0,102	11,13	319784,8036	6383837,92	47,649	57,5566	0,227858	-0,087413988
19GB100	0,102	11,15	319758,6338	6383838,57	46,89	57,5566	0,230595	-0,029666393
19GB101	0,26	11,17	319730,8785	6383837,41	46,0855	57,55658333	0,245757	-0,013075185
19GB102	0,408	11,19	319708,4885	6383837,72	45,467	57,55658333	0,266829	0,034643802
19GB103	0,533	11,21	319690,5135	6383835,36	44,85745	57,55656667	0,27053	0,045120734
19GB104	0,635	11,23	319650,385	6383831,1	44,29495	57,55653333	0,298644	0,067633894
19GB128	0,904	11,3	319612,8582	6383826,76	43,38945	57,5565	0,293623	0,157309158
19GB129	0,948	11,32	319585,6877	6383821,62	43,03645	57,55646667	0,192521	0,033815033
19GB130	0,992	11,34	319553,9662	6383817,07	42,70645	57,55643333	0,177998	0,001424017
19GB131	1,022	11,36	319534,0202	6383815,02	42,39245	57,55641667	0,147868	-0,058795274
19GB132	1,084	11,38	319504,1407	6383816,36	42,28845	57,55641667	0,140739	-0,024074983
19GB133	1,145	11,4	319476,3109	6383816,83	42,22695	57,55641667	0,12627	0,010665071
19GB134	1,159	11,43	319450,5703	6383817,97	42,05795	57,55641667	0,124482	-0,009906096
19GB135	1,127	11,45	319423,6321	6383823,25	42,05895	57,55643333	0,119967	-0,047286754
19GB136	1,166	11,47	319399,6804	6383827,67	41,87495	57,55645	0,12634	-0,039168967
19GB137	1,189	11,5	319371,3382	6383834,84	41,68395	57,55648333	0,129351	-0,0530055
19GB138	1,251	11,52	319347,7657	6383842,45	41,67495	57,55651667	0,140406	0,015848361
19GB139	1,303	11,54	319315,4197	6383854,04	41,54595	57,55656667	0,14618	0,044448711
19GB140	1,417	11,56	319292,0882	6383860,21	41,48295	57,5566	0,150184	0,14762976
19GB141	1,436	11,58	319266,6081	6383870,6	41,38595	57,55665	0,150062	0,143628524
19GB142	1,321	12,01	319239,2057	6383876,84	41,39745	57,55668333	0,142163	0,020713811
19GB143	1,37	12,04	319211,3045	6383885,33	41,15445	57,55671667	0,128844	0,006318872
19GB144	1,488	12,06	319186,3431	6383895,25	41,33645	57,55676667	0,120904	0,148379028
19GB145	1,759	12,08	319159,529	6383901,23	41,11045	57,55678333	0,127406	0,38036441
19GB146	2,11	12,15	319141,3199	6383909,4	41,07245	57,55683333	0,126108	0,71955781
19GB033	2,108	12,19	319118,1306	6383917,17	41,1455	57,55688333	0,106515	0,708840599
19GB032	1,994	12,21	319100,53	6383923,16	41,001	57,55688333	0,095655	0,555863528
19GB031f	1,84	12,24	319076,2297	6383930,37	41,11	57,55693333	0,07767	0,401672634
19GB147	1,755	12,26	319049,2593	6383940,55	41,151	57,55702	0,063123	0,303380433
19GB148	1,625	12,28	319020,6559	6383950,25	41,51	57,55705	0,055984	0,234699722
19GB149	1,62	12,33	318995,1171	6383959,45	41,873	57,55712	0,056905	0,297040679

			Instrument constant=	1		density=	2,67	

	BASE POINT							
	Reading	Time (h,min)	X-coordinate	Y-coordinate	Altitude (m)	Latitude (deg)		
Bas 1	2,295	13,33			39,424	57,56291315		
Bas 2	2,288	14,18						
Point	Reading	Time (h,min)	X-coordinate	Y-coordinate	Altitude (m)	Latitude (deg)	Terrain B-F	Dg (teor)
19GB166	2,376	13,38	318557,949	6384070,45	38,2705	57,55755	0,054133	0,349351834
19GB060	2,39	13,4	318549,3939	6384051,9	37,731	57,55746667	0,061865	0,272117417
19GB061	2,512	13,43	318512,2612	6384053,87	37,18	57,55746667	0,066785	0,291122218
19GB062	2,666	13,45	318479,7012	6384058,37	36,443	57,5575	0,072083	0,303026294
19GB063	2,585	13,48	318440,2822	6384064,12	35,7	57,55751667	0,074256	0,077149181
19GB064	2,468	13,5	318402,3612	6384069,48	35,247	57,55753333	0,084986	-0,1192834
19GB065	2,302	13,55	318354,4277	6384076,9	35,62	57,55751667	0,146023	-0,148730954
19GB066	2,269	13,59	318328,6196	6384081,5	36,398	57,55756667	0,06641	-0,111794266
19GB067	2,273	14,02	318277,2454	6384090,22	37,232	57,5576	0,037313	0,02488654
19GB068	2,357	14,05	318230,5734	6384101,02	37,643	57,55766667	0,029896	0,177306215
19GB069	2,465	14,08	318199,7477	6384102,44	38,391	57,55765	0,030408	0,434785159
19GB070	2,661	14,11	318160,1711	6384080,68	38,486	57,5575	n.a.	
			Instrument constant=	1		density=	2,67	
	BASE POINT							
	Reading	Time (h,min)	X-coordinate	Y-coordinate	Altitude (m)	Latitude (deg)		
Bas 1	2,288	14,18			39,424	57,56291315		
Bas 2	2,303	15,07						
Point	Reading	Time (h,min)	X-coordinate	Y-coordinate	Altitude (m)	Latitude (deg)	Terrain B-F	Dg (teor)
19GB150	1,606	14,25	318974,005	6383966,6	42,415	57,55715	0,058227	0,435592638
19GB151	1,719	14,29	318949,0834	6383975,92	42,8175	57,55717	0,060914	0,627584861
19GB152	1,669	14,32	318927,6308	6383984,09	43,299	57,55718	0,061422	0,67106461
19GB153	1,575	14,34	318897,1544	6383996,95	43,556	57,55725	0,073305	0,633139797
19GB154	1,625	14,36	318877,2767	6384005,33	43,571	57,5573	0,076926	0,684993671
19GB155	1,607	14,39	318849,2266	6384012,61	43,646	57,55733	0,085974	0,687412596
19GB156	1,509	14,41	318822,6662	6384017,21	43,452	57,55735	0,115819	0,57884334
19GB157	1,472	14,44	318792,7858	6384021,04	43,043	57,55738	0,142852	0,485044323
19GB158	1,507	14,46	318766,0552	6384023,59	42,407	57,55738	0,144185	0,395663687
19GB159	1,622	14,48	318742,9	6384026,83	41,568	57,5574	0,135602	0,334794739
19GB160	1,735	14,5	318716,1694	6384030,57	40,77	57,55742	0,13006	0,283031504
19GB161	1,854	14,52	318685,6931	6384034,83	40,202	57,55742	0,133115	0,292748489
19GB162	1,882	14,54	318657,2599	6384038,74	39,5945	57,55745	0,113957	0,179019587
19GB163	1,945	14,57	318634,3388	6384042,7	39,234	57,55743	0,109923	0,167798911
19GB164	2,075	15	318605,8205	6384046,36	38,7255	57,55745	0,079853	0,165146291
19GB165	2,219	15,03	318579,7709	6384050,36	38,2045	57,55747	0,069964	0,194215918
			Instrument constant=	1		density=	2,67	

	BASE POINT							
	Reading	Time (h,min)	X-coordinate	Y-coordinate	Altitude (m)	Latitude (deg)		
Bas 1	2,068	8,18			39,424	57,56291315		
Bas 2	1,996	9,38						
Point	Reading	Time (h,min)	X-coordinate	Y-coordinate	Altitude (m)	Latitude (deg)	Terrain B-F	Dg (teor)
19GB067	2,026	8,27						
19GB068	2,142	8,3						
19GB069	2,286	8,34						
20GB017	2,685	8,38	318148	6384076	38,1295	57,56249	0,044761	0,459873281
20GB016	2,462	8,41	318162	6384039	38,411	57,56217	0,034962	0,311417728
20GB015	2,363	8,45	318162	6383997	39,069	57,56179	0,029313	0,370996074
20GB014	2,392	8,48	318166	6383957	39,3645	57,56143	0,02791	0,48897471
20GB013	2,306	8,52	318178	6383917	39,6545	57,56107	0,026047	0,491311667
20GB012	2,195	8,55	318202	6383880	39,8995	57,56075	0,029873	0,461302159
20GB011	1,995	8,59	318218	6383846	39,8165	57,56045	0,029715	0,273049019
20GB010	1,885	9,04	318238	6383810	40,0865	57,56015	0,032122	0,247696205
20GB009	1,864	9,02	318241	6383792	40,289	57,55998	0,033354	0,279917695
20GB008	1,953	9,1	318241	6383751	40,613	57,55961	0,037174	0,474047203
20GB007	1,803	9,12	318254	6383713	41,296	57,55928	0,035842	0,485956099
20GB005	1,632	9,16	318302	6383653	41,8265	57,55876	0,042774	0,47253241
20GB004	1,444	9,19	318328	6383629	42,3675	57,55855	0,046384	0,414499506
20GB003	1,335	9,22	318331	6383596	43,0035	57,55826	0,057712	0,468439697
20GB002	1,496	9,25	318337	6383556	43,2105	57,5579	0,062258	0,706961049
20GB001	1,14	9,27	318328	6383527	45,4985	57,55764	0,10099	0,862891169
			Instrument constant=	1		density=	2,67	
	BASE POINT							
	Reading	Time (h,min)	X-coordinate	Y-coordinate	Altitude (m)	Latitude (deg)		
Bas 1	1,996	9,38			39,424	57,56291315		
Bas 2	1,931	10,55						
Point	Reading	Time (h,min)	X-coordinate	Y-coordinate	Altitude (m)	Latitude (deg)	Terrain B-F	Dg (teor)
20GB018	2,518	9,45	318120	6384098	39,104	57,56268	0,044619	0,528725693
20GB019	2,49	9,48	318081	6384105	39,6505	57,56273	0,056895	0,61892585
20GB020	2,566	9,51	318041	6384112	39,885	57,56277	0,082211	0,765616522
20GB021	2,655	9,54	317999	6384113	39,7935	57,56276	0,108525	0,866285916
20GB022	2,471	9,57	317959	6384113	40,237	57,56275	0,141012	0,80536297
20GB023	2,581	10	317921	6384113	40,124	57,56273	0,20363	0,959928313
20GB024	2,751	10,03	317880	6384109	39,9445	57,56268	0,191576	1,0892041
20GB025	2,786	10,07	317838	6384108	39,713	57,56266	0,169118	1,061228615
20GB026	2,872	10,09	317797	6384107	39,474	57,56263	0,176253	1,111503571
20GB027	2,84	10,12	317758	6384108	38,7825	57,56262	0,168575	0,939160787
20GB028	3,105	10,16	317717	6384104	37,999	57,56257	0,148842	1,037794757
20GB029	3,131	10,18	317678	6384100	37,119	57,56252	0,146882	0,894531839
20GB030	3,145	10,21	317639	6384093	36,215	57,56244	0,138705	0,731638298

20GB031	3,354	10,24	317602	6384083	34,9375	57,56234	0,136717	0,698108222
20GB032	3,51	10,27	317565	6384073	33,508	57,56223	0,120402	0,568173725
20GB033	3,467	10,3	317527	6384063	32,365	57,56212	0,10328	0,294786879
20GB034	3,282	10,34	317489	6384052	31,3605	57,56201	0,096001	-0,082669802
20GB035	2,995	10,41	317449	6384040	32,347	57,56189	0,079119	-0,176745687
20GB036	3,044	10,43	317430	6384079	33,8035	57,56223	0,072801	0,126204157
20GB037	2,873	10,46	317400	6384076	36,0815	57,56219	0,096429	0,432731953

			Instrument constant=	1		density=	2,67	
	BASE POINT							
	Reading	Time (h,min)	X-coordinate	Y-coordinate	Altitude (m)	Latitude (deg)		
Bas 1	1,538	9,27			39,424	57,56291315		
Bas 2	1,659	11,25						

Point	Reading	Time (h,min)	X-coordinate	Y-coordinate	Altitude (m)	Latitude (deg)	Terrain B-F	Dg (teor)
19GB001	0,166	9,38	319291,531	6384417,97	40,696	57,5596	0,113703	-0,747356287
19GB002	0,273	9,41	319273,5792	6384416,55	40,584333	57,5596	0,106957	-0,672143425
19GB003	0,377	9,44	319257,9693	6384413,71	40,488333	57,5596	0,100852	-0,596207925
19GB004	0,275	9,46	319236,9984	6384409,3	40,319333	57,55955	0,096524	-0,73372389
19GB005	0,343	9,49	319216,8159	6384410,87	40,391833	57,55953333	0,090581	-0,659113978
19GB006	0,348	9,52	319205,6209	6384402,04	40,234	57,55951667	0,088408	-0,689040702
19GB007	0,496	9,55	319184,8077	6384393,84	40,1975	57,55943333	0,099584	-0,533278469
19GB008	0,624	9,59	319164,7829	6384382,96	40,1155	57,55941667	0,146671	-0,377054174
19GB009	0,68	10,02	319153,1149	6384372,87	40,0125	57,55935	0,161911	-0,323676916
19GB010	0,531	10,05	319140,1855	6384362,78	39,911	57,55926667	0,138814	-0,511973184
19GB011	0,544	10,08	319122,5173	6384347,69	39,751	57,55918333	0,091236	-0,57425741
19GB012	0,504	10,12	319107,2312	6384336,61	39,606	57,55916667	0,066823	-0,669925229
19GB013	0,451	10,14	319096,1939	6384327,46	39,5145	57,55905	0,055529	-0,744689206
19GB014	0,364	10,18	319084,9989	6384316,58	39,3875	57,55898333	0,052474	-0,858353146
19GB015	0,32	10,21	319070,0197	6384297,35	39,313	57,5589	0,053036	-0,912679465
19GB016	0,385	10,3	319060,9779	6384278,87	39,26	57,5588	0,049985	-0,862173833
19GB017	0,41	10,33	319050,4333	6384261,39	39,1435	57,5587	0,051545	-0,853395115
19GB018	0,485	10,36	319040,4975	6384237,42	39,0095	57,55856667	0,042979	-0,805447772
19GB019	0,575	10,39	319032,2398	6384218,83	38,8495	57,55846667	0,039109	-0,745655486
19GB020	0,674	10,41	319018,9328	6384188,71	38,4305	57,5583	0,038626	-0,717922386
19GB021	0,687	10,45	319017,829	6384166,48	37,9455	57,55818333	0,039099	-0,794371644

19GB022	0,748	10,48	319030,2066	6384142,51	37,339	57,55806667	0,04827	-0,836996546
19GB023	0,759	10,51	319052,36	6384121,62	37,10525	57,55795	0,054689	-0,859053393
19GB024	0,787	10,53	319070,2562	6384101,67	36,90475	57,55785	0,050939	-0,868081963
19GB025	0,756	10,57	319084,233	6384081,62	37,49575	57,55775	0,051099	-0,778563079
19GB026	0,688	11	319096,2727	6384053,26	38,02275	57,5576	0,056758	-0,728003215
19GB027	0,841	11,04	319101,7126	6384026,38	38,02425	57,55745	0,056785	-0,566466753
19GB028	1,074	11,06	319099,3474	6384001,47	38,00075	57,55728333	0,058907	-0,324333459
19GB029	1,333	11,09	319091,779	6383973,48	37,92975	57,5572	0,063227	-0,071213138
19GB030	1,254	11,11	319082,9491	6383944,07	37,80675	57,55695	0,074057	-0,145101128

			Instrument constant=	1		density=	2,67	

BASE POINT

	Reading	Time (h,min)	X-coordinate	Y-coordinate	Altitude (m)	Latitude (deg)
Bas 1	1,62	9,22			39,424	57,56291315
Bas 2	1,575	10,19				

Point	Reading	Time (h,min)	X-coordinate	Y-coordinate	Altitude (m)	Latitude (deg)	Terrain B-F	Dg (teor)
19GB106	0,427	9,31	319115,6094	6384308,31	42,409	57,55896667	0,05307	-0,221656892
19GB107	0,302	9,35	319135,5567	6384293,49	42,256	57,5589	0,055388	-0,365802443
19GB119	0,279	9,38	319154,74	6384312,59	42,4005	57,559	0,063537	-0,358072377
19GB120	0,266	9,4	319172,8172	6384331,07	42,4535	57,5591	0,069709	-0,361106848
19GB121	0,377	9,43	319191,3439	6384343,51	42,4315	57,55918333	0,076845	-0,251771936
19GB108	0,437	9,46	319154,9465	6384276,91	41,8115	57,55881667	0,061345	-0,296752382
19GB109	0,42	9,49	319172,1736	6384262,87	41,944	57,55873333	0,059967	-0,279857029
19GB110	0,411	9,52	319196,7885	6384254,64	42,6065	57,5587	0,071416	-0,141988799
19GB111	0,493	9,54	319217,5939	6384260,4	43,1445	57,55873333	0,118199	0,09146105
19GB112	0,423	9,58	319224,4598	6384282,73	42,823	57,55886667	0,092353	-0,075413626
19GB113	0,351	10	319234,359	6384308,59	42,823	57,559	0,089894	-0,159241079
19GB114	0,417	10,04	319212,0886	6384236,34	43,6095	57,5586	0,088737	0,096306874
19GB115	0,469	10,06	319212,1437	6384212,04	43,4775	57,55848333	0,088635	0,133398418
19GB116	0,513	10,08	319217,1273	6384184,06	43,0935	57,55833333	0,074888	0,102013381
19GB117	0,547	10,1	319217,4378	6384154,72	42,7375	57,55816667	0,086514	0,092877424
19GB118	0,596	10,12	319200,6892	6384141,87	41,8455	57,5581	0,093126	-0,019914526

			Instrument constant=	1		density=	2,67	

BASE POINT

	Reading	Time (h,min)	X-coordinate	Y-coordinate	Altitude (m)	Latitude (deg)		
Bas 1	1,575	10,19			39,424	57,56291315		
Bas 2	1,724	10,53						

Point	Reading	Time (h,min)	X-coordinate	Y-coordinate	Altitude (m)	Latitude (deg)	Terrain B-F	Dg (teor)
19GB122	3,592	10,3	318775,9149	6385451,14	35,554	57,5717	0,097761	0,583974264
19GB123	3,485	10,32	318809,1845	6385455,08	35,406	57,57173333	0,069097	0,407697632
19GB124	3,312	10,34	318843,5578	6385441,6	35,903	57,57166667	0,073583	0,333651541
19GB125	3,201	10,36	318874,2061	6385422,19	36,7	57,57156667	0,099414	0,404696834
19GB126	3,443	10,4	318905,9186	6385415,58	37,604	57,57155	0,120582	0,829520638
19GB127	3,823	10,43	318927,3625	6385444,91	36,007	57,57171667	0,121521	0,869500771

			Instrument constant=	1		density=	2,67	

BASE POINT

	Reading	Time (h,min)	X-coordinate	Y-coordinate	Altitude (m)	Latitude (deg)		
Bas 1	1,832	7,32			39,424	57,56291315		
Bas 2	1,85	8,48						

Point	Reading	Time (h,min)	X-coordinate	Y-coordinate	Altitude (m)	Latitude (deg)	Terrain B-F	Dg (teor)
20GB038	-2,773	7,46	322968	6382553	49,063	57,55074	0,037377	
20GB039	-2,664	7,48	322938	6382512	48,548	57,55036	0,054475	
20GB040	-2,379	7,51	322923	6382481	47,0525	57,55008	0,033856	
20GB041	-2,207	7,54	322918	6382454	46,0085	57,54984	0,050895	
20GB042	-1,961	7,56	322933	6382424	44,5045	57,54957	0,048748	
20GB043f	-1,973	7,59	322928	6382410	44,3455	57,54945	0,055863	
20GB044	-2,477	8,02	322943	6382383	47,0395	57,54921	0,06857	
20GB045	-2,89	8,05	322965	6382351	49,3105	57,54893	0,078204	
20GB046	-3,014	8,09	322970	6382320	49,6095	57,54865	0,078493	
20GB047	-3	8,12	322985	6382288	49,5125	57,54837	0,095835	
20GB048	-3,815	8,15	323000	6382253	53,9935	57,54807	0,132282	
20GB049	-3,811	8,18	323001	6382219	53,8795	57,54776	0,127266	
20GB050	-4,196	8,21	323013	6382184	55,866	57,54745	0,138993	
20GB051	-3,794	8,23	323030	6382148	53,4845	57,54713	0,127382	
20GB052	-3,754	8,26	323046	6382121	52,3665	57,54689	0,087122	
20GB043f	-1,968	8,32						

			Instrument constant=	1		density=	2,67	

BASE POINT

	Reading	Time (h,min)	X-coordinate	Y-coordinate	Altitude (m)	Latitude (deg)		
Bas 1	1,798	9,19			39,424	57,56291315		
Bas 2	1,763	11,14						

Point	Reading	Time (h,min)	X-coordinate	Y-coordinate	Altitude (m)	Latitude (deg)	Terrain B-F	Dg (teor)
20GB043f	-2,024	9,35						

20GB053	-4,099	9,42	323052	6382093	53,6045	57,54665	0,141674	
20GB054	-4,621	9,45	323063	6382083	56,9325	57,54656	0,151038	
20GB055	-5,192	9,47	323072	6382068	60,1485	57,54643	0,148713	
20GB056	-5,652	9,5	323069	6382054	62,6675	57,54631	0,162062	
20GB057	-6,035	9,52	323073	6382035	64,8225	57,54613	0,157199	
20GB058	-6,431	9,54	323075	6382010	67,1775	57,54591	0,170917	
20GB059	-6,773	9,57	323083	6381990	68,9115	57,54573	0,182195	
20GB060	-6,689	9,59	323085	6381965	68,5865	57,54551	0,173465	
20GB061	-6,497	10,02	323087	6381937	67,5495	57,54526	0,156369	
20GB062	-6,287	10,04	323096	6381918	66,2505	57,54509	0,14829	
20GB063	-5,948	10,07	323108	6381891	64,2975	57,54485	0,165075	
20GB064	-5,513	10,1	323117	6381868	61,5875	57,54466	0,177433	
20GB065	-5,043	10,12	323123	6381850	58,7635	57,54449	0,185034	
20GB066	-4,47	10,16	323135	6381836	55,3435	57,54438	0,210729	
20GB067	-4,045	10,18	323132	6381816	52,9795	57,54419	0,197127	
20GB068	-3,645	10,21	323141	6381808	50,8775	57,54412	0,172054	
20GB069	-2,775	10,27	323157	6381758	46,202	57,54374	0,136261	
20GB070	-2,337	10,3	323166	6381740	43,564	57,54352	0,139474	
20GB071	-2,128	10,32	323177	6381723	42,62	57,54338	0,136224	
20GB072	-1,878	10,35	323186	6381696	41,244	57,54314	0,115743	
20GB073	-1,803	10,37	323189	6381665	40,736	57,54287	0,106861	
20GB043f	-2,57	10,57						

			Instrument constant=	1		density=	2,67	
	BASE POINT							
	Reading	Time (h,min)	X-coordinate	Y-coordinate	Altitude (m)	Latitude (deg)		
Bas 1	1,974	7,3			39,424	57,56291315		
Bas 2	1,876	9,05						

Point	Reading	Time (h,min)	X-coordinate	Y-coordinate	Altitude (m)	Latitude (deg)	Terrain B-F	Dg (teor)
20GB074	2,634	8,58	317382	6384055	35,231	57,56199	0,116306	0,118111957
20GB075	2,485	8,55	317354	6384039	36,174	57,56184	0,125175	0,172689833
20GB076	2,507	8,53	317317	6384031	37,142	57,56175	0,199504	0,464750718
20GB077	2,481	8,51	317279	6384021	37,827	57,56165	0,241419	0,621552447
20GB078	2,589	8,49	317243	6384011	37,51	57,56154	0,17602	0,608767509
20GB079	2,593	8,46	317206	6383995	37,709	57,56139	0,132245	0,617356452
20GB080	2,862	8,44	317174	6383977	36,037	57,56121	0,110176	0,548119815
20GB081	3,052	8,42	317141	6383956	34,787	57,56101	0,06446	0,460885803
20GB082	3,194	8,39	317105	6383944	33,649	57,56089	0,080832	0,402170463
20GB083	3,308	8,37	317071	6383951	33,014	57,56094	0,075793	0,380058471
20GB084	3,368	8,35	317032	6383955	32,381	57,56096	0,071526	0,307574967
20GB085	3,422	8,33	316994	6383953	32,033	57,56092	0,072363	0,295181218
20GB086	3,433	8,3	316955	6383945	32,051	57,56083	0,066468	0,308121349
20GB087	3,435	8,28	316920	6383938	32,01	57,56076	0,074855	0,31412769
20GB088	3,248	8,26	316877	6383951	33,116	57,56086	0,083517	0,343066764
20GB089	3,357	8,23	316844	6383962	32,087	57,56094	0,115382	0,271864188
20GB090	3,455	8,21	316828	6383993	31,437	57,56121	0,113724	0,21612012

20GB091	3,518	8,19	316793	6383992	30,844	57,56119	0,143292	0,191623733
20GB092	3,946	8,16	316760	6384011	28,31	57,56134	0,172024	0,134507077
20GB093	4,234	8,14	316725	6384020	26,351	57,56141	0,208764	0,066100874
20GB094	4,458	8,12	316686	6384006	24,288	57,56127	0,260752	-0,054272681
20GB095	4,76	8,09	316649	6384017	22,407	57,56136	0,212893	-0,180608892
20GB096	4,865	8,06	316611	6384025	22,185	57,56141	0,161573	-0,177796208
20GB097	4,875	8,04	316574	6384033	22,313	57,56147	0,13686	-0,174320857
20GB098	4,658	8,02	316540	6384043	23,821	57,56155	0,148553	-0,091635128
20GB099	5,385	7,58	316500	6384054	19,057	57,56163	0,173522	-0,28744083
20GB100	5,566	7,55	316464	6384056	17,995	57,56163	0,197045	-0,294908285
20GB101	5,857	7,52	316431	6384043	16,025	57,5615	0,219431	-0,361443354
20GB102	5,967	7,49	316402	6384026	14,2375	57,56134	0,303098	-0,509336526
20GB103	6,191	7,46	316377	6383996	13,0875	57,56106	0,21993	-0,574815913
20GB104	5,999	7,43	316351	6383983	14,3375	57,56093	0,219088	-0,514203916

			Instrument constant=	1		density=	2,67	
	BASE POINT							
	Reading	Time (h,min)	X-coordinate	Y-coordinate	Altitude (m)	Latitude (deg)		
Bas 1	2,29	9,22			39,424	57,56291315		
Bas 2	2,272	10,3						

Point	Reading	Time (h,min)	X-coordinate	Y-coordinate	Altitude (m)	Latitude (deg)	Terrain B-F	Dg (teor)
22GB004	2,615	9,29	318380	6384807	41,382	57,56914	0,242436	0,443228334
22GB032	4,519	9,38	318355	6385134	32,526	57,57206	0,109205	0,234699163
22GB031	4,738	9,41	318330	6385107	30,596	57,57181	0,162592	0,148770746
22GB030	4,847	9,44	318312	6385071	29,503	57,57149	0,14757	0,054817773
22GB029	4,838	9,47	318299	6385035	29,208	57,57115	0,180353	0,04927856
22GB028	4,796	9,49	318299	6385002	29,329	57,57086	0,22503	0,100091638
22GB027	4,588	9,52	318299	6384961	29,751	57,57049	0,362491	0,143727528
22GB026	4,425	6,56	318295	6384920	30,277	57,57012	0,367219	0,072705079
22GB001	4,293	9,58	318289	6384888	30,495	57,56984	0,271221	-0,041250366
22GB002	4,125	10	318291	6384855	30,84	57,56953	0,261904	-0,124728086
22GB003	4,091	10,02	318296	6384831	31,005	57,56932	0,261052	-0,109355906
22GB006	4,009	10,05	318297	6384793	31,305	57,56898	0,210185	-0,154507457
22GB007	3,913	10,08	318305	6384760	31,674	57,56869	0,163739	-0,199770159
22GB008	3,869	10,11	318313	6384717	32,088	57,56831	0,162898	-0,131187871
22GB009	3,732	10,13	318320	6384680	32,434	57,56798	0,161896	-0,17351139
22GB010	3,721	10,16	318328	6384645	32,932	57,56767	0,154888	-0,06731949
22GB011	3,677	10,19	318335	6384603	33,277	57,5673	0,143393	-0,02378395

22GB012	3,432	10,22	318337	6384589	33,389	57,56717	0,136003	-0,242677121
			Instrument constant=	1		density=	2,67	
	BASE POINT							
	Reading	Time (h,min)	X-coordinate	Y-coordinate	Altitude (m)	Latitude (deg)		
Bas 1	2,272	10,3			39,424	57,56291315		
Bas 2	2,248	11,25						
Point	Reading	Time (h,min)	X-coordinate	Y-coordinate	Altitude (m)	Latitude (deg)	Terrain B-F	Dg (teor)
22GB013	3,105	10,38	318351	6384553	33,77	57,56685	0,118916	-0,479942434
22GB014	2,91	10,41	318361	6384520	34,121	57,56656	0,102418	-0,597281945
22GB015	2,887	10,43	318364	6384479	34,19	57,56619	0,083022	-0,59485753
22GB016	2,751	10,46	318371	6384436	34,832	57,56581	0,113388	-0,541704333
22GB017	2,735	10,49	318379	6384399	35,145	57,56548	0,098656	-0,482468184
22GB018	2,769	10,51	318369	6384362	35,178	57,56514	0,075344	-0,436503365
22GB019	2,653	10,54	318354	6384331	35,793	57,56486	0,067716	-0,414864312
22GB020	2,496	10,59	318340	6384295	36,269	57,56453	0,083216	-0,433460868
22GB021	2,421	11,03	318324	6384258	36,642	57,56419	0,063753	-0,424895789
22GB022	2,357	11,05	318305	6384228	36,941	57,56392	0,049951	-0,420845029
22GB023	2,229	11,1	318281	6384202	37,361	57,56368	0,050216	-0,44408032
22GB024	2,226	11,15	318251	6384179	37,729	57,56345	0,055168	-0,348677945
22GB025	2,391	11,18	318218	6384160	37,89	57,56327	0,05511	-0,135980177
			Instrument constant=	1		density=	2,67	
	BASE POINT							
	Reading	Time (h,min)	X-coordinate	Y-coordinate	Altitude (m)	Latitude (deg)		
Bas 1	2,137	13,21			39,424	57,56291315		
Bas 2	2,121	14,29						
Point	Reading	Time (h,min)	X-coordinate	Y-coordinate	Altitude (m)	Latitude (deg)	Terrain B-F	Dg (teor)
22GB33	7,31	13,34	316535	6385077	10,765	57,57082	0,045597	-1,064690381
22GB34	7,253	13,36	316571	6385073	11,357	57,5708	0,084884	-0,963844422
22GB35	7,224	13,39	316597	6385045	11,407	57,57056	0,049868	-0,997617961
22GB36	7,162	13,42	316635	6385055	11,753	57,57066	0,058246	-0,990684769
22GB37	6,971	13,45	316673	6385067	13,063	57,57078	0,088146	-0,903252269
22GB38	6,891	13,48	316705	6385082	13,62	57,57093	0,080926	-0,892517762

22GB39	7,126	13,51	316742	6385093	12,076	57,57105	0,143122	-0,908171875
22GB40	6,851	13,54	316771	6385102	13,881	57,57114	0,18685	-0,791081987
22GB41f	6,575	13,58	316795	6385139	15,604	57,57148	0,201971	-0,740015456
22GB42	6,536	14	316820	6385167	15,459	57,57175	0,249378	-0,781823334
22GB43	6,56	14,04	316845	6385197	15,383	57,57203	0,199445	-0,844749086
22GB44	6,596	14,06	316868	6385227	15,609	57,5723	0,165533	-0,819899954
22GB45	6,592	14,08	316895	6385254	15,703	57,57256	0,084962	-0,906853291
22GB46	6,723	14,12	316933	6385252	14,873	57,57255	0,144114	-0,87820049
22GB47	6,715	14,15	316966	6385242	14,756	57,57247	0,21095	-0,83510555
22GB48	6,482	14,18	316999	6385228	16,181	57,57236	0,221796	-0,767226112
			Instrument constant=	1		density=	2,67	
	BASE POINT							
	Reading	Time (h,min)	X-coordinate	Y-coordinate	Altitude (m)	Latitude (deg)		
Bas 1	1,722	8,22			39,424	57,56291315		
Bas 2	1,697	10,25						
Point	Reading	Time (h,min)	X-coordinate	Y-coordinate	Altitude (m)	Latitude (deg)	Terrain B-F	Dg (teor)
21GB001	6,942	8,37	316831	6386136	12,018	57,58044	0,053226	-1,553246773
21GB002	6,783	8,42	316846	6386101	12,045	57,58013	0,03926	-1,694441724
21GB003	6,926	8,48	316886	6386095	11,654	57,58009	0,041779	-1,621329939
21GB004	7,09	8,51	316926	6386097	11,7065	57,58012	0,052196	-1,438438735
21GB005	7,138	8,55	316964	6386109	11,9225	57,58025	0,054302	-1,355702494
21GB006	6,843	8,58	317001	6386110	12,1345	57,58027	0,038289	-1,626046816
21GB007	6,71	9,03	317038	6386106	12,5685	57,58025	0,032484	-1,676826084
21GB008	6,543	9,07	317069	6386096	12,9265	57,58017	0,026705	-1,771807197
21GB009	6,502	9,11	317107	6386080	13,0945	57,58005	0,027185	-1,768619267
21GB010	6,683	9,14	317104	6386043	12,9415	57,57972	0,022222	-1,594982058
21GB011	6,835	9,18	317105	6386007	12,7925	57,5794	0,021517	-1,445917434
21GB012	6,998	9,21	317101	6385970	12,7145	57,57906	0,020286	-1,27097463
21GB013	7,02	9,24	317106	6385933	12,7535	57,57873	0,018159	-1,215734528
21GB014	7,119	9,27	317105	6385896	12,6475	57,57839	0,016646	-1,110581029
21GB015	7,233	9,31	317102	6385857	12,5785	57,57804	0,017733	-0,979525413
21GB016	7,129	9,34	317100	6385837	12,5335	57,57787	0,015657	-1,079889546
21GB017	6,807	9,37	317094	6385802	12,342	57,57755	0,015554	-1,412785146

21GB018	6,538	9,41	317097	6385767	12,151	57,57724	0,012562	-1,696088819
21GB019	6,421	9,44	317099	6385729	11,928	57,57689	0,013276	-1,826900763
21GB020	6,502	9,48	317104	6385689	11,787	57,57654	0,014763	-1,742606868
21GB021	6,538	9,53	317116	6385655	12,007	57,57624	0,013254	-1,639200872
21GB022	6,436	9,56	317123	6385618	12,021	57,57591	0,0152	-1,708804036
21GB023	6,376	10	317132	6385586	12,224	57,57562	0,018227	-1,701229778
21GB024	6,337	10,03	317135	6385565	12,1595	57,57544	0,027822	-1,727937183
21GB025	6,292	10,08	317139	6385548	12,2855	57,57529	0,02777	-1,734876145
21GB026	6,22	10,11	317147	6385538	12,6355	57,5752	0,022644	-1,735159745
21GB027	6,198	10,14	317111	6385523	12,4815	57,57505	0,021131	-1,776042248
								9780318,46
			Instrument constant=	1		density=	2,67	
	BASE POINT							
	Reading	Time (h,min)	X-coordinate	Y-coordinate	Altitude (m)	Latitude (deg)		
Bas 1	1,697	10,25			39,424	57,56291315		
Bas 2	1,76	12,25						

Point	Reading	Time (h,min)	X-coordinate	Y-coordinate	Altitude (m)	Latitude (deg)	Terrain B-F	Dg (teor)
21GB028	6,214	10,37	317102	6385490	12,43	57,57475	0,028247	-1,742495275
21GB029	6,354	10,4	317089	6385454	12,471	57,57443	0,039116	-1,55886948
21GB030	6,646	10,43	317078	6385419	12,516	57,57411	0,065625	-1,206816747
21GB031	6,658	10,46	317063	6385386	12,768	57,5738	0,141116	-1,045885772
21GB032	6,579	10,49	317049	6385355	12,967	57,57352	0,134365	-1,071084368
21GB033	6,498	10,52	317037	6385329	13,238	57,57328	0,13535	-1,079667894
21GB034	6,412	10,54	317026	6385281	14,085	57,57285	0,183873	-0,916292473
21GB035	6,206	10,57	317014	6385243	15,311	57,5725	0,185881	-0,851974389
21GB036	5,845	11,01	317025	6385213	17,4855	57,57224	0,201291	-0,750596813
21GB037	4,667	11,16	317046	6385140	25,7715	57,57159	0,203716	-0,250830796
21GB038	4,358	11,23	317068	6385116	27,4725	57,57139	0,194014	-0,222202832
21GB039	4,206	11,27	317095	6385095	28,3455	57,57121	0,148347	-0,235474447
21GB040	4,079	11,3	317112	6385066	29,2525	57,57095	0,114917	-0,197729053
21GB041	3,9	11,33	317105	6385030	30,6575	57,57063	0,109311	-0,081277427
21GB042	3,673	11,35	317111	6384995	32,4925	57,57032	0,108013	0,075767561
21GB043	3,639	11,38	317111	6384957	32,6405	57,56997	0,08472	0,074742902
21GB044	3,503	11,43	317127	6384919	32,1815	57,56964	0,086172	-0,125625502

21GB045	3,234	11,46	317128	6384882	34,1035	57,56931	0,083038	0,005813655
21GB046	3,206	11,49	317115	6384851	34,6425	57,56903	0,072023	0,094230838
21GB047	3,137	11,52	317107	6384815	34,9335	57,5687	0,055299	0,091262073
21GB048	3,212	11,55	317104	6384776	35,3405	57,56835	0,044266	0,262443547
21GB049	3,149	11,57	317104	6384739	35,6495	57,56801	0,042084	0,284903622
21GB050	3,167	12	317114	6384707	35,9345	57,56773	0,040372	0,378662413
21GB051	3,218	12,03	317120	6384671	36,2705	57,56741	0,031268	0,511344792
21GB052	3,176	12,05	317124	6384636	36,4355	57,5671	0,029474	0,52440561
21GB053	3,07	12,08	317133	6384599	36,1745	57,56677	0,031277	0,394386129
21GB054	3,073	12,1	317142	6384575	36,3935	57,56656	0,03198	0,457356487
21GB055	2,953	12,13	317149	6384549	36,8535	57,56633	0,024942	0,438107588
21GB056	3,012	12,16	317158	6384514	35,7245	57,56602	0,039207	0,313172664

			Instrument constant=	1		density=	2,67	
	BASE POINT							
	Reading	Time (h,min)	X-coordinate	Y-coordinate	Altitude (m)	Latitude (deg)		
Bas 1	1,691	13,1			39,424	57,56291315		
Bas 2	1,672	14,22						

Point	Reading	Time (h,min)	X-coordinate	Y-coordinate	Altitude (m)	Latitude (deg)	Terrain B-F	Dg (teor)
21GB057	3,13	13,23	317170	6384481	34,5615	57,56573	0,076643	0,331359684
21GB058	2,813	13,27	317184	6384446	36,6365	57,56542	0,035248	0,407623325
21GB059	2,583	13,29	317202	6384419	38,1825	57,56518	0,029571	0,496276051
21GB060	2,747	13,31	317215	6384382	37,6235	57,56485	0,034267	0,582636503
21GB061	2,509	13,34	317227	6384346	39,0795	57,56454	0,037997	0,661004132
21GB062	2,501	13,36	317253	6384318	39,7305	57,5643	0,079118	0,842408372
21GB063	2,294	13,39	317272	6384292	40,8175	57,56408	0,079464	0,868420934
21GB064	2,031	13,41	317300	6384275	42,3315	57,56393	0,099454	0,936057778
21GB065	1,989	13,44	317326	6384248	42,3135	57,5637	0,070374	0,881111609
21GB066	2,302	13,47	317344	6384220	40,2325	57,56346	0,071862	0,806761786
21GB067	2,358	13,49	317375	6384197	39,4795	57,56326	0,066403	0,726135159
21GB068	2,43	13,53	317397	6384171	38,6575	57,56304	0,069541	0,658703043
21GB069	2,324	13,54	317411	6384136	38,3915	57,56273	0,106759	0,563313725
21GB070	2,391	13,56	317408	6384100	37,975	57,5624	0,114241	0,583491048
21GB071	2,272	14,05	317380	6384019	35,2935	57,56167	0,056753	-0,058139806
21GB072	2,209	14,08	317376	6383985	35,3305	57,56136	0,044416	-0,099955589
21GB073	2,266	14,11	317374	6383950	35,4925	57,56105	0,036754	0,007491294
21GB074	2,278	14,13	317378	6383913	35,4705	57,56072	0,033654	0,039685623
21GB075	2,387	14,16	317387	6383876	35,4415	57,56039	0,047679	0,184892085

			Instrument constant=	1		density=	2,67	
	BASE POINT							
	Reading	Time (h,min)	X-coordinate	Y-coordinate	Altitude (m)	Latitude (deg)		
Bas 1	1,672	14,22			39,424	57,56291315		
Bas 2	1,644	15,1						

Point	Reading	Time (h,min)	X-coordinate	Y-coordinate	Altitude (m)	Latitude (deg)	Terrain B-F	Dg (teor)
21GB076	2,437	14,28	317395	6383837	35,5395	57,56004	0,072727	0,313036376
21GB077	2,349	14,3	317401	6383800	36,0295	57,55972	0,087877	0,364009547
21GB078	2,246	14,33	317408	6383765	36,4055	57,5594	0,090378	0,365493353
21GB079	2,213	14,35	317419	6383730	36,6735	57,55909	0,095183	0,416633278
21GB080	2,241	14,38	317439	6383697	36,8935	57,5588	0,09427	0,512554935
21GB081	2,343	14,42	317458	6383667	36,4395	57,55854	0,094271	0,548934854
21GB082	2,581	14,45	317479	6383635	35,0885	57,55827	0,086551	0,537391425
21GB083	2,706	14,47	317498	6383603	33,7965	57,55799	0,074597	0,420457144
21GB084	2,858	14,49	317512	6383571	32,7905	57,5577	0,076606	0,401563326
21GB085	2,959	14,52	317541	6383558	31,6555	57,5576	0,122012	0,334675206
21GB086	2,79	14,54	317551	6383526	31,5715	57,55732	0,113295	0,164592138
21GB087	2,711	14,56	317565	6383489	31,4625	57,557	0,11517	0,093467989
21GB088	2,947	14,59	317578	6383455	31,3945	57,55669	0,121774	0,349899937
21GB089	3,058	15,01	317592	6383418	31,3205	57,55637	0,095018	0,447029567

			Instrument constant=	1		density=	2,67	
	BASE POINT							
	Reading	Time (h,min)	X-coordinate	Y-coordinate	Altitude (m)	Latitude (deg)		
Bas 1	1,644	15,1			39,424	57,56291315		
Bas 2	1,675	15,48						

Point	Reading	Time (h,min)	X-coordinate	Y-coordinate	Altitude (m)	Latitude (deg)	Terrain B-F	Dg (teor)
21GB114	6,38	15,2	317089	6386101	13,6695	57,58023	0,027426	-1,73216674
21GB115	6,488	15,23	317097	6386143	13,8775	57,58061	0,027621	-1,616694651
21GB116	6,655	15,25	317109	6386178	14,2825	57,58092	0,029447	-1,395280291
21GB117	6,787	15,27	317127	6386209	14,7285	57,58121	0,033721	-1,196711575
21GB118	6,73	15,29	317145	6386240	14,5985	57,5815	0,029324	-1,309113119
21GB119	6,546	15,31	317168	6386269	14,6505	57,58176	0,035157	-1,500022845
21GB120	6,51	15,33	317190	6386297	14,7775	57,58203	0,045243	-1,524747706
21GB121	6,441	15,35	317217	6386320	15,1965	57,58224	0,053558	-1,521882518
21GB122	6,401	15,37	317248	6386334	16,0755	57,58238	0,066355	-1,38930794

			Instrument constant=	1		density=	2,67	
	BASE POINT							
	Reading	Time (h,min)	X-coordinate	Y-coordinate	Altitude (m)	Latitude (deg)		
Bas 1	1,582	10,24			39,424	57,56291315		
Bas 2	1,515	11,49						

Point	Reading	Time (h,min)	X-coordinate	Y-coordinate	Altitude (m)	Latitude (deg)	Terrain B-F	Dg (teor)

21GB113	1,489	10,36	317695	6385029	62,4355	57,56752	0,208375	4,272993611
21GB112	1,523	10,39	317725	6385007	63,1125	57,56766	0,199636	4,422292264
21GB111	1,311	10,41	317762	6384985	62,4735	57,5677	0,165176	4,048433489
21GB110	1,174	11,43	317796	6384960	62,0495	57,56758	0,11345	3,835028418
21GB109	1,171	10,46	317829	6384929	62,3875	57,56751	0,114819	3,86069929
21GB108	1,411	10,49	317864	6384904	63,4645	57,56753	0,139501	4,337950338
21GB107	1,9	10,52	317889	6384875	66,739	57,56778	0,229908	5,543293706
21GB106	2,008	10,53	317889	6384847	67,597	57,56797	0,192887	5,768232017
21GB105	1,712	10,56	317863	6384841	66,331	57,56816	0,157834	5,174923409
21GB104	1,157	11	317834	6384833	63,128	57,56826	0,166736	3,993737976
21GB103	0,805	11,03	317805	6384824	61,106	57,56839	0,194065	3,263031587
21GB102	0,735	11,05	317784	6384811	60,671	57,56863	0,211461	3,106737169
21GB101	0,629	11,08	317778	6384777	60,669	57,56894	0,146975	2,912773838
21GB100	0,927	11,09	317809	6384749	62,43	57,56906	0,18689	3,588015251
21GB099	1,365	11,13	317849	6384734	64,674	57,56916	0,164637	4,440101472
21GB098	1,31	11,16	317882	6384721	64,619	57,56924	0,167928	4,373371315
21GB097	0,998	11,21	317913	6384699	62,583	57,56931	0,182121	3,673277261
21GB096	0,707	11,24	317938	6384677	60,46	57,56958	0,159457	2,922218526
21GB095	0,457	11,27	317952	6384650	58,596	57,56984	0,132053	2,259186176
21GB094	0,252	11,3	317931	6384650	57,194	57,57006	0,13402	1,764684081
21GB093	0,117	11,32	317912	6384660	56,797	57,57033	0,126221	1,523207099
21GB092	0,179	11,34	317887	6384674	55,37	57,57054	0,124795	1,287427305
21GB091	0,631	11,36	317861	6384671	52,753	57,57073	0,141518	1,227365008
21GB090	0,807	11,38	317837	6384657	51,474	57,57092	0,137482	1,13372876

Appendix II

Table with point ID, gravimeter reading, coordinates in SWEREF99, altitude, latitude, terrain correction constant and corrected gravity value. This is the data produced during this project.

			Instrument constant=	**1**		**density=**	**2,67**	
	BASE POINT							
	Reading	Time (h,min)	X-coordinate	Y-coordinate	Altitude (m)	Latitude (deg)		
Bas 1	1,455	13,17			39,424	57,56291315		
Bas 2	1,468	14,22						
Point	Reading	Time (h,min)	X-coordinate	Y-coordinate	Altitude (m)	Latitude (deg)	Terrain B-F	Dg (teor)
23GB001	2,081	14,15	318141	6384189	39,355	57,5635	0,135612	981768,6708
23GB002	1,918	14,11	318170	6384216	39,542	57,56376	0,071443	981769,8819
23GB003	1,901	14,07	318151	6384243	41,33	57,56399	0,073443	981770,9529
23GB004	1,552	14,03	318118	6384265	42,919	57,56418	0,077793	981771,8375
23GB005	1,268	13,56	318087	6384284	44,566	57,56433	0,090447	981772,5358
23GB006	0,739	13,51	318064	6384300	47,821	57,56447	0,146444	981773,1874
23GB007	0,295	13,48	318032	6384318	50,15	57,56462	0,168356	981773,8855
23GB008	-0,666	13,4	318005	6384343	56,305	57,56483	0,1502	981774,8626
23GB009	-1,043	13,35	317978	6384363	59,061	57,56499	0,123886	981775,6069
23GB010	-1,209	13,33	317961	6384375	60,201	57,5651	0,153104	981776,1186
23GB011	-1,469	13,3	317923	6384378	61,938	57,56511	0,093817	981776,1651
23GB012	-1,733	13,26	317902	6384392	63,565	57,56522	0,112407	981776,6767
			Instrument constant=	1		density=	2,67	
	BASE POINT							
	Reading	Time (h,min)	X-coordinate	Y-coordinate	Altitude (m)	Latitude (deg)		
Bas 1	1,591	16,41			39,424	57,56291315		
Bas 2	1,574	17,33						
Point	Reading	Time (h,min)	X-coordinate	Y-coordinate	Altitude (m)	Latitude (deg)	Terrain B-F	Dg (teor)
23GB013	0,602	17,21	318725	6384789	50,622	57,56912	0,075756	981794,7791
23GB014	0,611	17,19	318754	6384795	49,988	57,56918	0,066001	981795,057
23GB015	0,547	17,16	318789	6384814	49,972	57,56937	0,064796	981795,9371
23GB016	0,48	17,14	318827	6384810	50,0059	57,56935	0,065414	981795,8445
23GB017	0,519	17,11	318865	6384830	50,0429	57,56954	0,081275	981796,7244
23GB018	0,588	17,08	318900	6384836	50,2679	57,56961	0,061671	981797,0485
23GB019	0,593	17,04	318939	6384830	50,7169	57,56957	0,055046	981796,8633
23GB020	0,636	17,01	318973	6384828	50,1849	57,56957	0,058092	981796,8633
23GB021	0,536	16,58	319018	6384819	49,6339	57,56951	0,060814	981796,5854
23GB022	0,245	16,54	319063	6384833	49,8309	57,56965	0,100385	981797,2337

			Instrument constant=	1		density=	2,67	
	BASE POINT							
	Reading	Time (h,min)	X-coordinate	Y-coordinate	Altitude (m)	Latitude (deg)		
Bas 1	1,583	15,06			39,424	57,56291315		
Bas 2	1,591	16,41						
Point	Reading	Time (h,min)	X-coordinate	Y-coordinate	Altitude (m)	Latitude (deg)	Terrain B-F	Dg (teor)
23GB023	0,419	16,26	319078	6384863	49,9849	57,56993	0,147545	981798,5299
23GB024			319079	6384887	50,1019	57,57014	0,13608	
23GB025	0,44	16,22	319098	6384931	50,5359	57,57055	0,132017	981801,3989
23GB026	0,384	16,19	319110	6384966	51,1629	57,57086	0,090685	981802,8327
23GB027	0,391	16,15	319145	6384985	51,1519	57,57105	0,146172	981803,7112
23GB028	0,213	16,11	319181	6384994	52,0369	57,57114	0,158472	981804,1273
23GB029	-0,05	16,06	319218	6384996	53,1139	57,57117	0,254441	981804,266
23GB030	-0,025	16,03	319252	6385004	52,8329	57,57126	0,122042	981804,6821
23GB031	-0,134	15,59	319293	6385002	53,5249	57,57126	0,114182	981804,6821
23GB032	-0,025	15,56	319323	6384990	51,6389	57,57116	0,155929	981804,2198
23GB033	-0,25	15,52	319351	6384981	52,7439	57,57109	0,187131	981803,8962
23GB034	-1,109	15,49	319388	6384981	58,1229	57,57111	0,14582	981803,9886
23GB035	-1,298	15,46	319409	6384974	58,4199	57,57105	0,149435	981803,7112
23GB036	-1,526	15,4	319454	6384988	59,7469	57,57119	0,16578	981804,3585
23GB037	-2,063	15,36	319485	6384996	63,2289	57,57128	0,161553	981804,7745
23GB038	-2,339	15,33	319489	6385026	65,0799	57,57155	0,202758	981806,0224
23GB039	-2,442	15,28	319498	6385051	65,7659	57,57177	0,357781	981807,0389

			Instrument constant=	1		density=	2,67	
	BASE POINT							
	Reading	Time (h,min)	X-coordinate	Y-coordinate	Altitude (m)	Latitude (deg)		
Bas 1	1,526	14,27			39,424	57,56291315		
Bas 2	1,535	15,56						
Point	Reading	Time (h,min)	X-coordinate	Y-coordinate	Altitude (m)	Latitude (deg)	Terrain B-F	Dg (teor)
23GB040	-3,19	14,47	319588	6384997	68,018	57,57133	0,420077	981805,0056
23GB041	-2,938	14,5	319619	6384978	66,636	57,57117	0,289647	981804,266
23GB042	-3,234	14,54	319647	6384970	68,233	57,57111	0,32473	981803,9886
23GB043	-3,444	14,57	319666	6384949	69,832	57,57093	0,289405	981803,1564
23GB044	-3,729	15,01	319699	6384941	71,586	57,57087	0,222884	981802,8789
23GB045	-3,838	15,03	319722	6384913	72,383	57,57063	0,106124	981801,7689
23GB046	-3,772	15,06	319762	6384927	71,624	57,57077	0,161718	981802,4165
23GB047	-3,733	15,09	319804	6384930	71,755	57,57081	0,15076	981802,6014
23GB048	-3,732	15,12	319845	6384936	71,876	57,57088	0,180609	981802,9252
23GB049	-3,413	15,15	319877	6384916	69,675	57,57072	0,206632	981802,1852
23GB050	-2,87	15,21	319907	6384890	65,75	57,5705	0,20289	981801,1676
23GB051	-2,626	15,23	319940	6384875	63,619	57,57037	0,224539	981800,5661
23GB052	-2,446	15,26	319978	6384872	62,01	57,57036	0,274782	981800,5199

23GB053	-2,22	15,29	320020	6384854	60,2	57,57022	0,283994	981799,8721
23GB054	-2,235	15,32	320037	6384833	59,746	57,57003	0,28787	981798,9928
23GB055	-2,292	15,35	320068	6384809	59,047	57,56984	0,282334	981798,1133
23GB056	-2,294	15,38	320095	6384794	57,9625	57,56971	0,282997	981797,5115
23GB057	-2,314	15,4	320135	6384784	57,6235	57,56964	0,194198	981797,1874
23GB058	-2,367	15,43	320169	6384779	57,5895	57,5696	0,217772	981797,0022
23GB059	-2,643	15,45	320206	6384772	59,6645	57,56956	0,262562	981796,817

			Instrument constant=	1		density=	2,67	
	BASE POINT							
	Reading	Time (h,min)	X-coordinate	Y-coordinate	Altitude (m)	Latitude (deg)		
Bas 1	1,535	15,56			39,424	57,56291315		
Bas 2	1,523	16,47						

Point	Reading	Time (h,min)	X-coordinate	Y-coordinate	Altitude (m)	Latitude (deg)	Terrain B-F	Dg (teor)
23GB060	-2,969	16,07	320221	6384809	62,2565	57,56989	0,186252	981798,3448
23GB061	-2,835	16,1	320232	6384845	61,9605	57,57022	0,19062	981799,8721
23GB062	-2,771	16,12	320248	6384881	61,6625	57,57055	0,17429	981801,3989
23GB063	-2,709	16,16	320252	6384922	61,7945	57,57092	0,138183	981803,1101
23GB064	-2,587	16,18	320237	6384960	60,9485	57,57126	0,119045	981804,6821
23GB065	-2,607	16,22	320266	6384985	60,8885	57,57149	0,137695	981805,7451
23GB066	-2,724	16,24	320303	6384993	61,2925	57,57158	0,180077	981806,161
23GB067	-3,095	16,26	320342	6384992	63,9805	57,57159	0,260943	981806,2072
23GB068	-3,185	16,28	320375	6385007	64,3915	57,57174	0,191665	981806,9003
23GB069	-3,278	16,31	320407	6385031	64,9125	57,57196	0,187744	981807,9167
23GB070	-3,392	16,36	320444	6385047	66,0145	57,57211	0,179686	981808,6095

			Instrument constant=	1		density=	2,67	
	BASE POINT							
	Reading	Time (h,min)	X-coordinate	Y-coordinate	Altitude (m)	Latitude (deg)		
Bas 1	1,49	11,19			39,424	57,56291315		
Bas 2	1,457	12,44						

Point	Reading	Time (h,min)	X-coordinate	Y-coordinate	Altitude (m)	Latitude (deg)	Terrain B-F	Dg (teor)
23GB071	-3,559	11,33	320454	6385078	66,1065	57,5724	0,154182	981809,9487
23GB072	-3,673	11,36	320486	6385121	66,301	57,5728	0,237287	981811,7952
23GB073	-3,873	11,39	320504	6385149	67,8455	57,57306	0,261024	981812,995
23GB074	-4,379	11,42	320520	6385165	71,1575	57,57321	0,261976	981813,687
23GB075	-4,923	11,46	320531	6385198	74,8625	57,57351	0,257654	981815,0708
23GB076	-6,741	11,5	320570	6385284	87,2095	57,5743	0,10658	981818,7127
23GB077	-6,92	11,54	320586	6385317	88,4245	57,5746	0,121297	981820,0949
23GB078	-6,918	11,57	320604	6385350	88,4435	57,5749	0,14884	981821,4767
23GB079	-6,46	12	320632	6385362	85,8395	57,57502	0,11857	981822,0293
23GB080	-6,455	12,03	320669	6385361	85,824	57,57502	0,12456	981822,0293

23GB081	-6,428	12,06	320705	6385353	85,252	57,57497	0,21518	981821,7991
23GB082	-6,98	12,09	320747	6385323	88,532	57,57471	0,146168	981820,6016
23GB083	-7,418	12,12	320761	6385302	90,869	57,57453	0,120721	981819,7725
23GB084	-7,655	12,14	320784	6385297	92,476	57,5745	0,062571	981819,6342
23GB085	-7,782	12,18	320812	6385296	93,614	57,5745	0,05512	981819,6342
23GB086	-7,33	12,21	320841	6385320	91,334	57,57472	0,086527	981820,6477
23GB087	-7,002	12,24	320861	6385333	89,698	57,57485	0,156042	981821,2465

			Instrument constant=	1		density=	2,67	
	BASE POINT							
	Reading	Time (h,min)	X-coordinate	Y-coordinate	Altitude (m)	Latitude (deg)		
Bas 1	1,468	14,22			39,424	57,56291315		
Bas 2	1,468	14,55						

Point	Reading	Time (h,min)	X-coordinate	Y-coordinate	Altitude (m)	Latitude (deg)	Terrain B-F	Dg (teor)
23GB088	1,396	14,32	318094	6384315	50,471	57,56461	0,078649	981773,839
23GB089	1,949	14,35	318096	6384347	48,424	57,5649	0,107755	981775,1883
23GB090	1,22	14,39	318094	6384390	46,554	57,56528	0,146821	981776,9557
23GB091			318087	6384412	48,287	57,56548	0,172326	

Appendix III

Step by step guide on how to convert a DEM from TIFF to ascii in preparation for the terrain correction program made by Prof. E. Sturkell:

1. Download a DEM in *.TIF format from maps.slu.se
2. Import the*.TIF file into Qgis
3. Use the tool “Raster pixels to points”. It produces a vector with the height for each pixel in the form of a shapefile.
4. Then the tool “Add X/Y fields to layer” is used. This tool adds columns with the X and Y coordinates to the shapefile.
5. Lastly, the shapefile can be exported to *.CSV format.